

33 Years of Polar Aeronomy in Svalbard

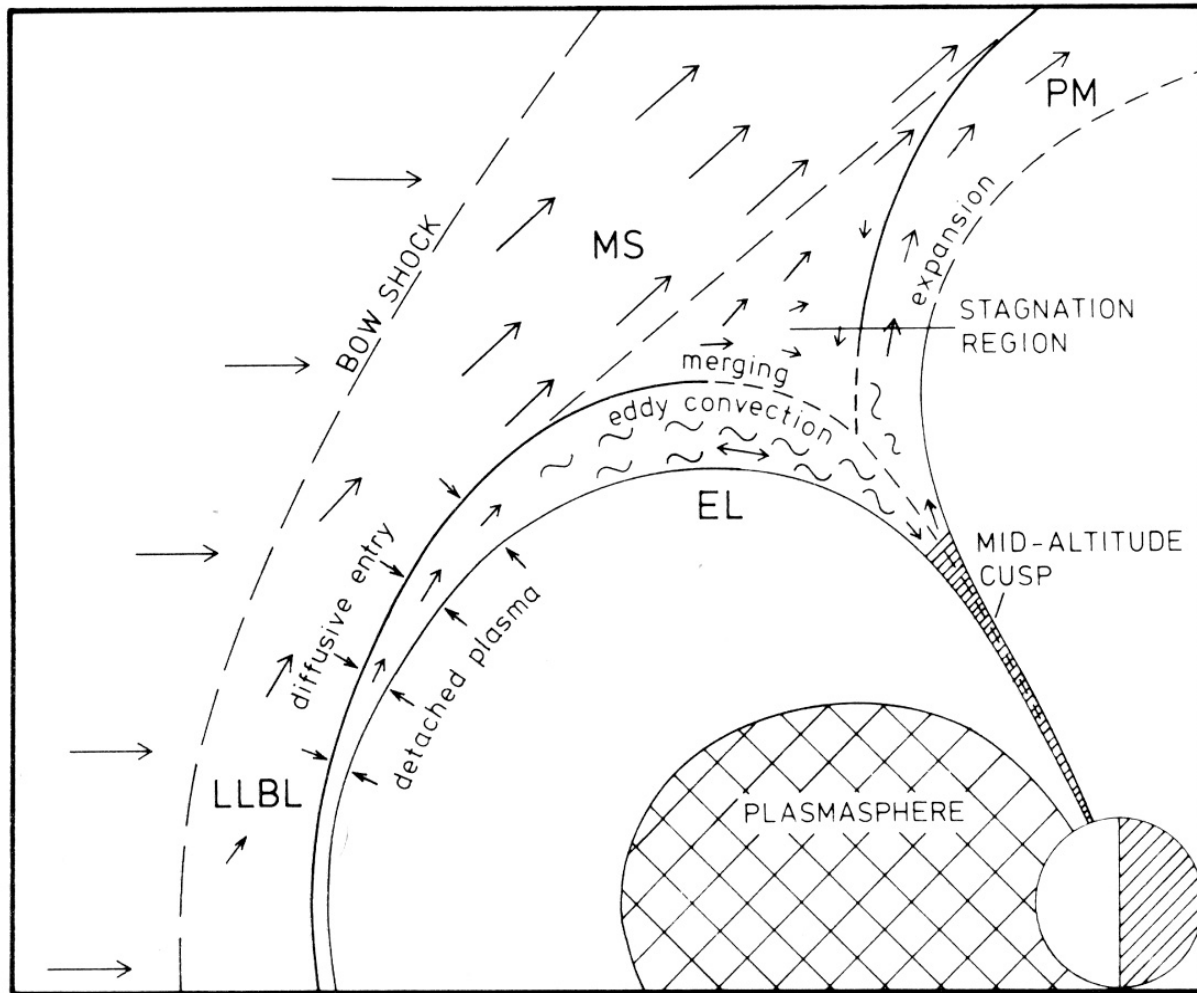
A review of scientific adventures north of 78°
by

Charles Deehr

Prof. Emer. Phys.

The Geophysical Institute
University of Alaska Fairbanks

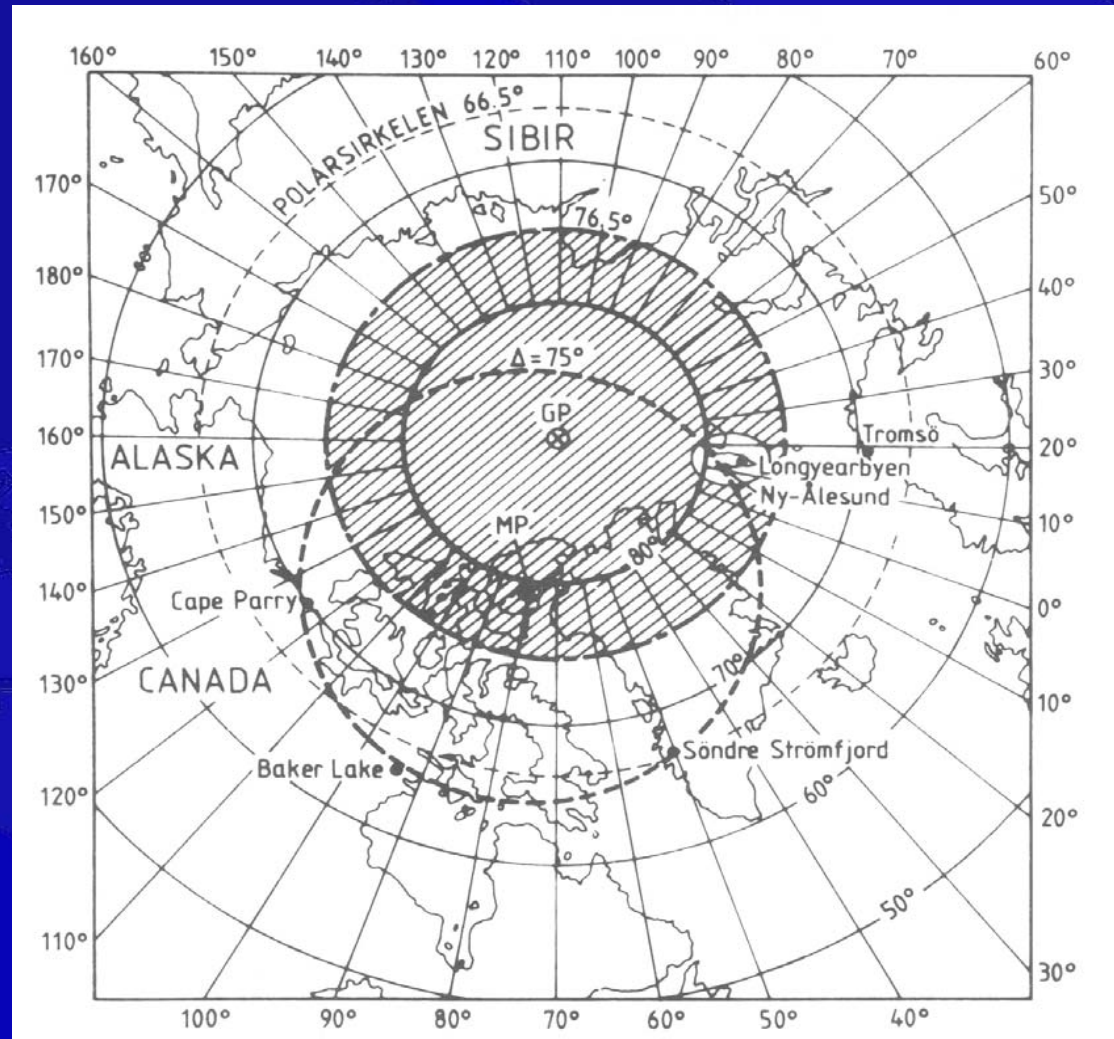
Magnetospheric Cusps



- Magnetosphere has two cavities toward the sun.
- Concave singularity points

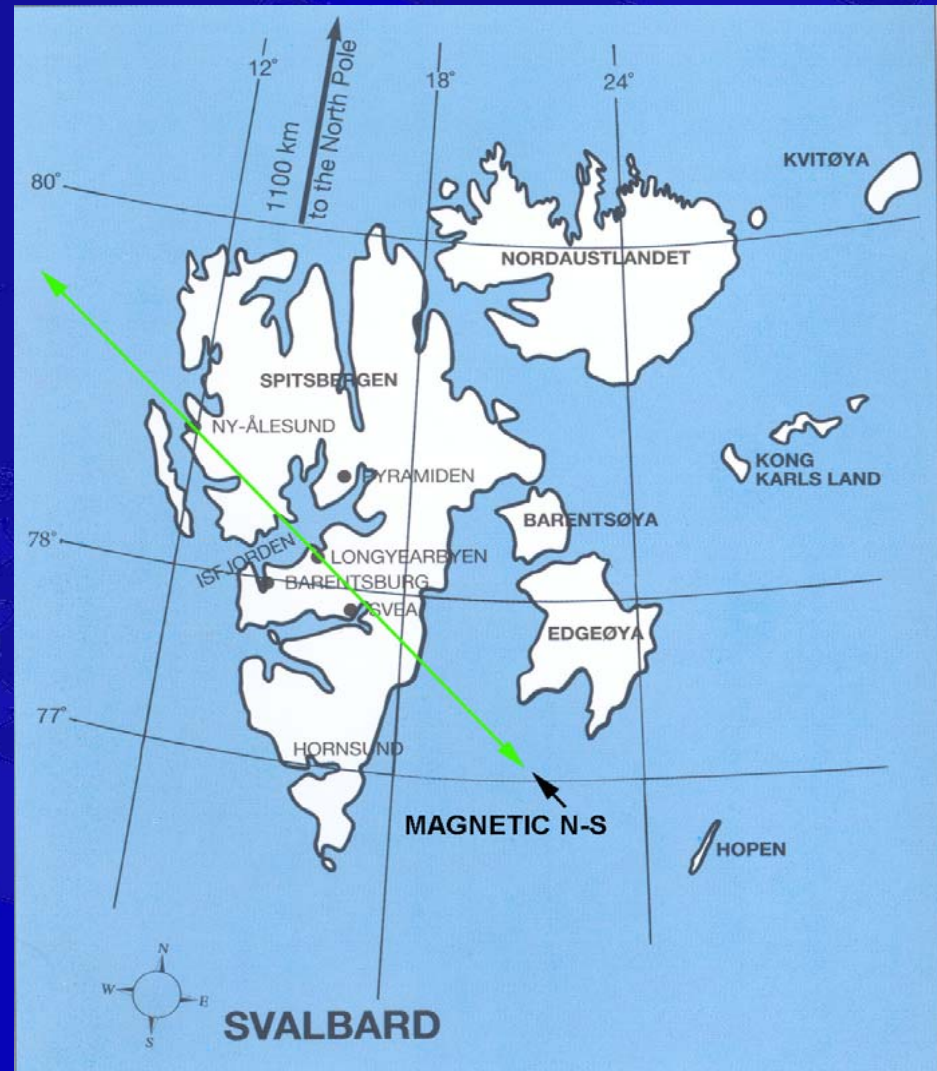
Magnetospheric Cusp

- Footpoint of cusp is near 75° magnetic latitude.
- Sun is $>10^\circ$ below horizon in shaded area during northern winter.
- Svalbard and Franz Josef Land only observatories



Location of Observatories

- Locations of outlying stations allowed some larger coverage.
- Ny Aalesund a major scientific station in geomag. meridian.
- Hopen and Hornsund secondary stations.



Access to Svalbard

- From 1596, the islands were accessible only by ship.
- Last ship out in Dec., first ship in in May.
- Daily commercial jet service established in 1975



Longyearbyen



- A coal mining town from 1914.
- Now mainly tourist with hotels, etc.

Dayside Aurora from Svalbard 1970

- Establishing an Auroral Observatory at Longyearbyen, October 1970
- Egeland, Omholt arrange UiO Physics Dept sponsor hut construction and transport to Breinosa.



EISCAT on Breinosa 1996



- Hut on Breinosa in 1970 replaced by EISCAT
- Northern Lights Station moved to valley (arrow)

34 Years of Polar Aeronomy in Svalbard

Dayside Aurora from Svalbard 1978

- U of Tromsø, U of Oslo, U of Alaska, NSF establish Nordlysstasjonen I Adventdalen, Summer 1978.



Dayside Aurora from Svalbard 1978

Multi-national Svalbard Auroral Expedition - 1978-79



34 Years of Polar Aeronomy in Svalbard

Dayside Observations Early 1980s

- Soviet stations at Barentsberg, Grumantbyen and Pyramiden
- Visits
- Here is bust of Lenin and a look-alike in Barentsberg.



Dayside Aurora from Svalbard 1978

- Instruments outdoors led to stressful maintenance.



Dayside Aurora from Svalbard 1980

- Polar bears outdoors led to stressful maintenance.



Three Years at LYR

- Headlines in the local newspaper "Auroral researchers in Adventdalen for the third year in a row"



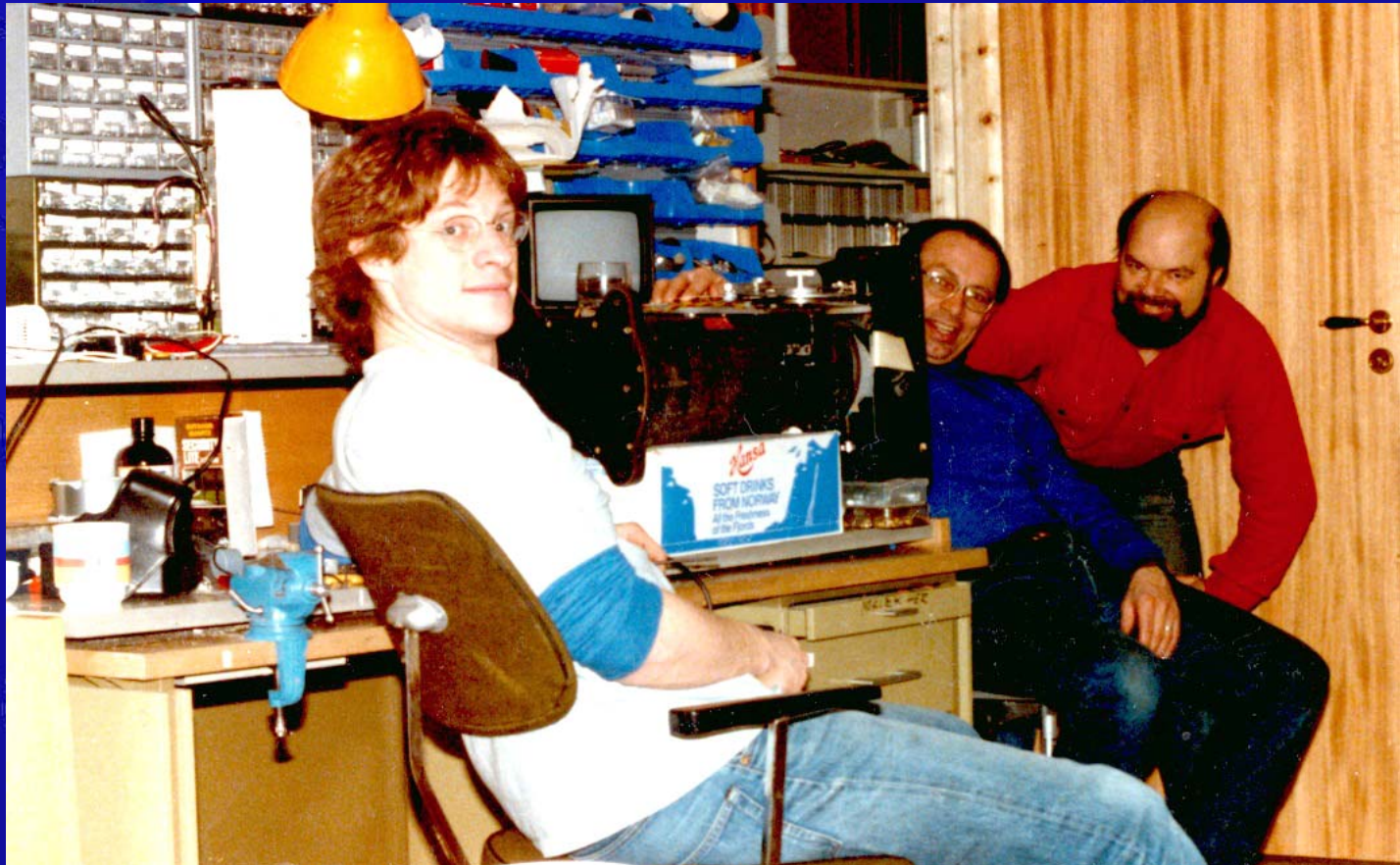
Dayside Aurora from Svalbard - 1984

- Permanent station built 1984, expanded 1988.



Dayside Aurora from Svalbard - 1984

- Calibration and observation in warmth and comfort.



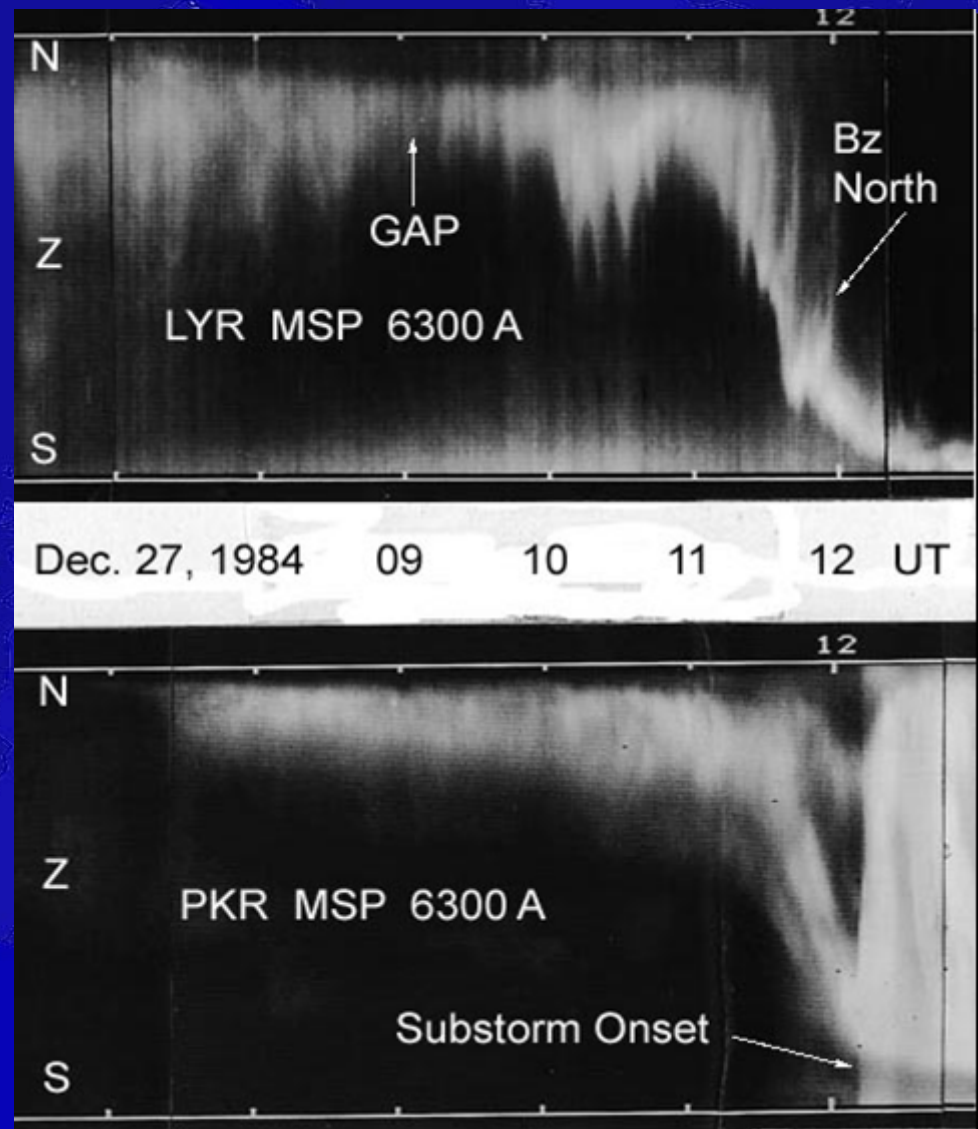
Dayside Aurora from Svalbard - 1988

- Permanent station expanded in 1988, used as command center for rocket launches from SvalRak and Andoya.

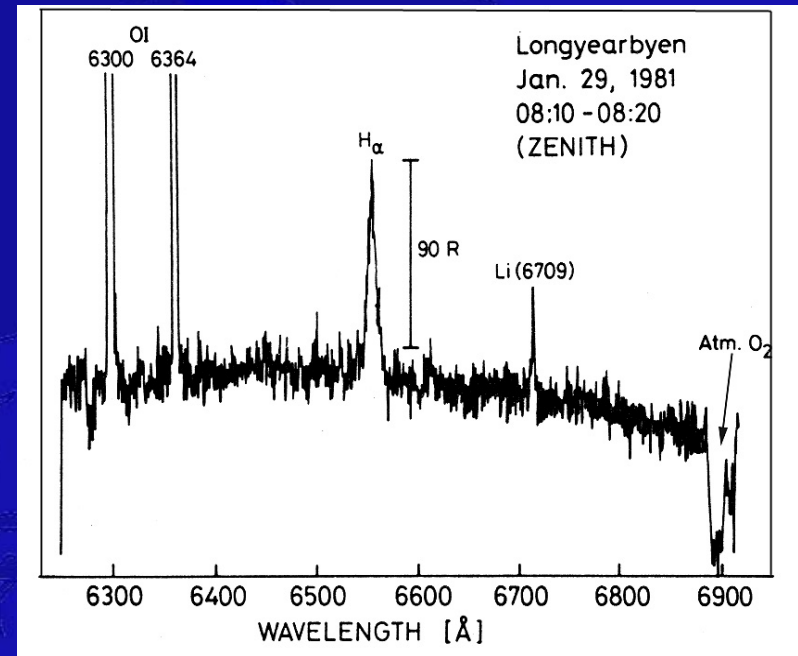
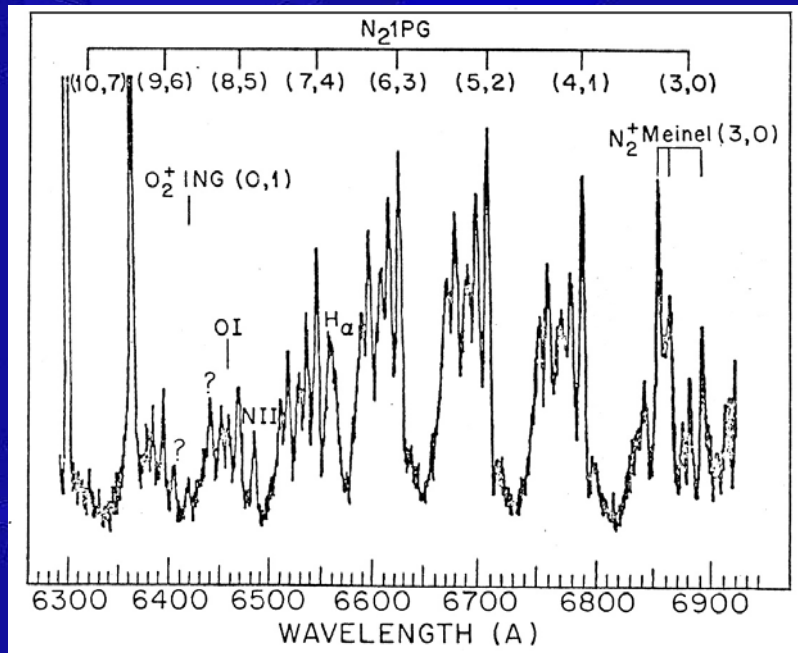


Simultaneous from Svalbard & Alaska

- IMF Bz southward turning begins equatorward movement simultaneously on day and night side.
- There is aurora in the “Dayside Gap”
- A northward motion of the dayside aurora occurs within 15 min of all substorm onsets.



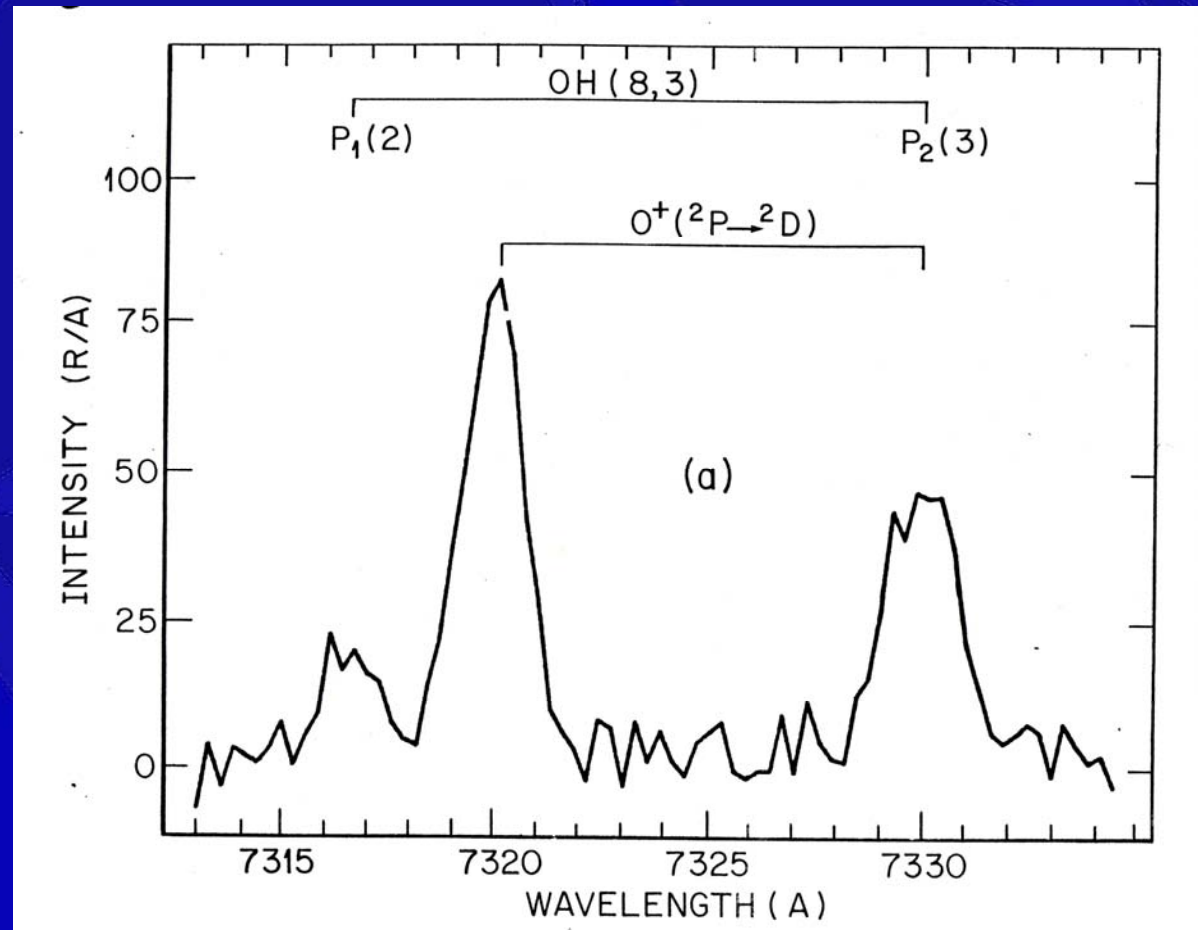
Auroral Emission Spectra



Dayside auroral spectra were almost devoid of molecular bands, allowing new view of atomic emissions in the aurora. It was like a great red aurora every day for about an hour.

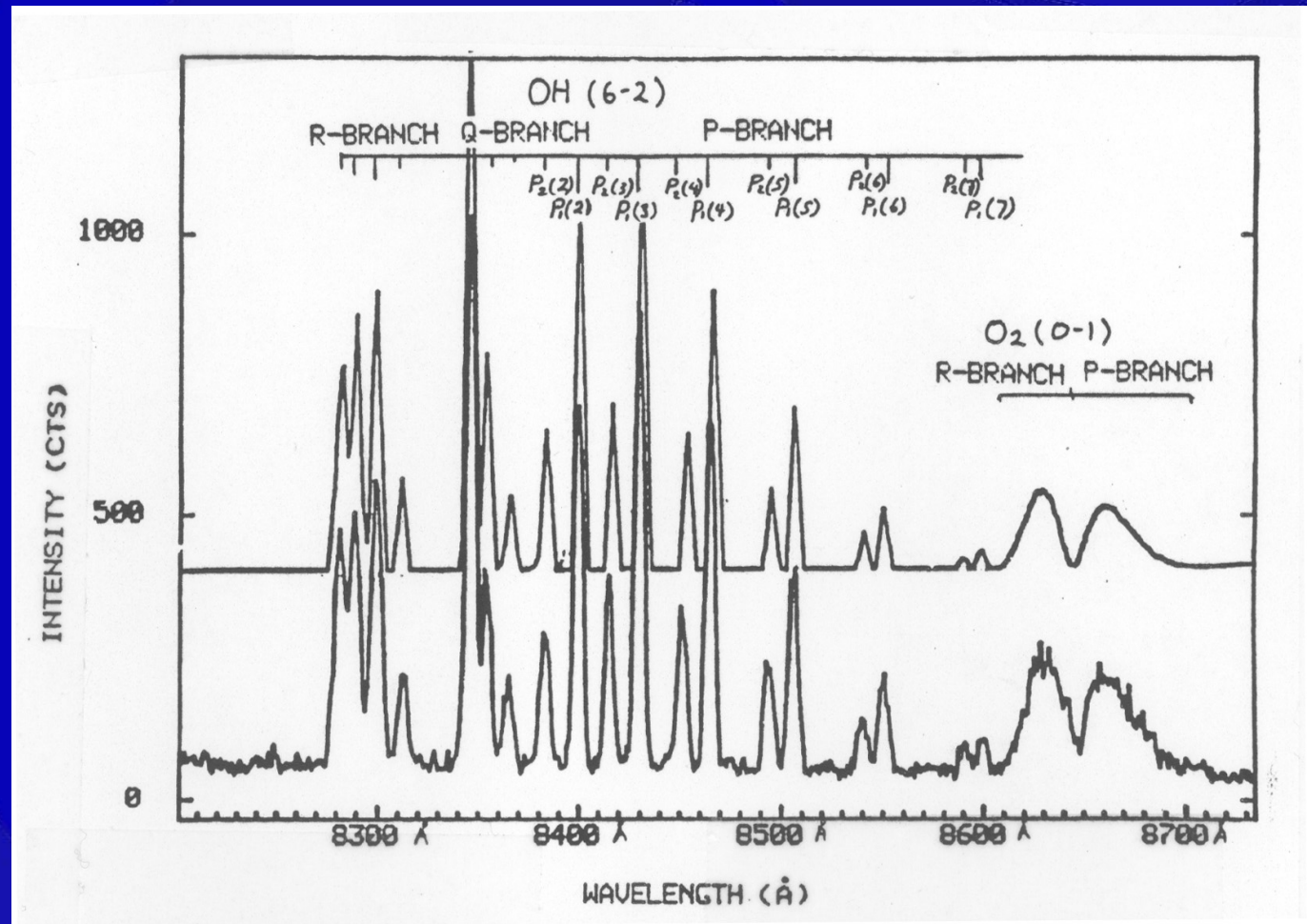
F-region Neutral and Ion Winds

- Roger Smith and students from Ireland used Fabry-Perot measurements of Doppler shifted atomic lines to measure winds.



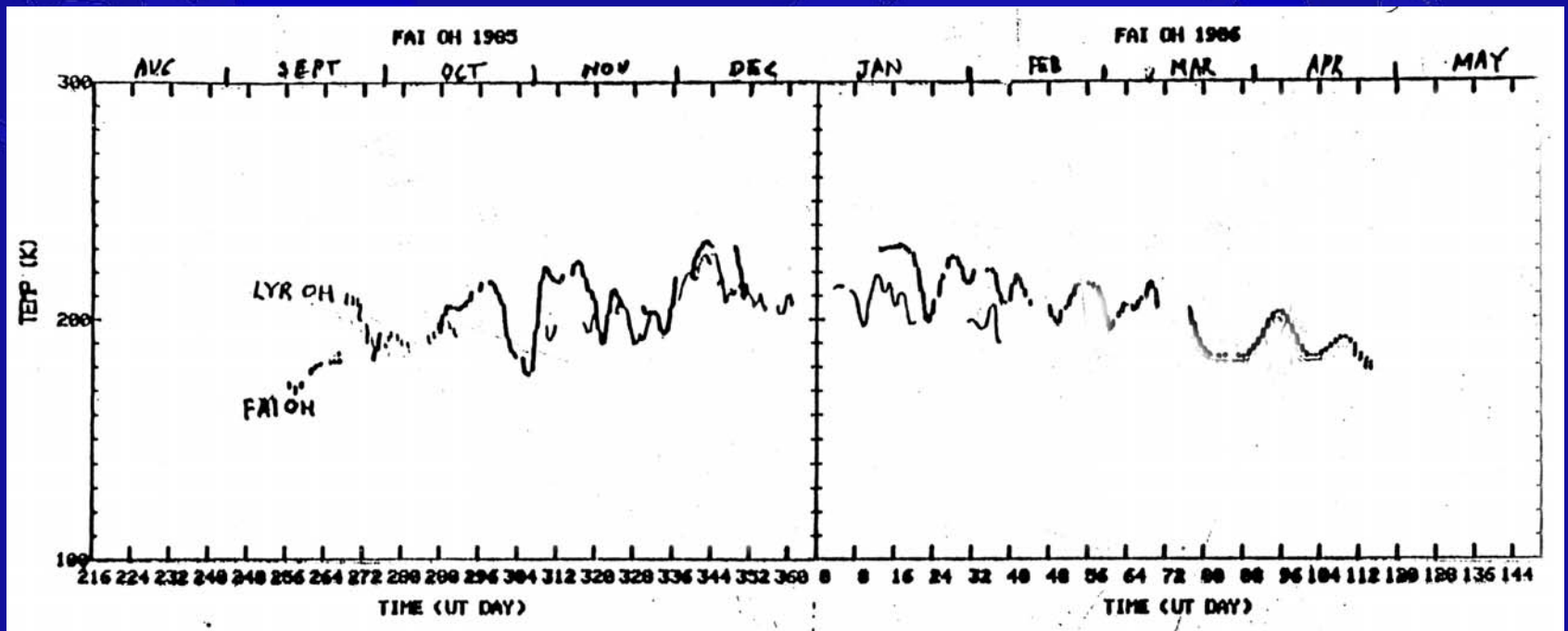
OH and O₂ Airglow

- Polar airglow emissions from the 85 & 100 km altitude regions.
- Temperature measured from relative emission line intensities.



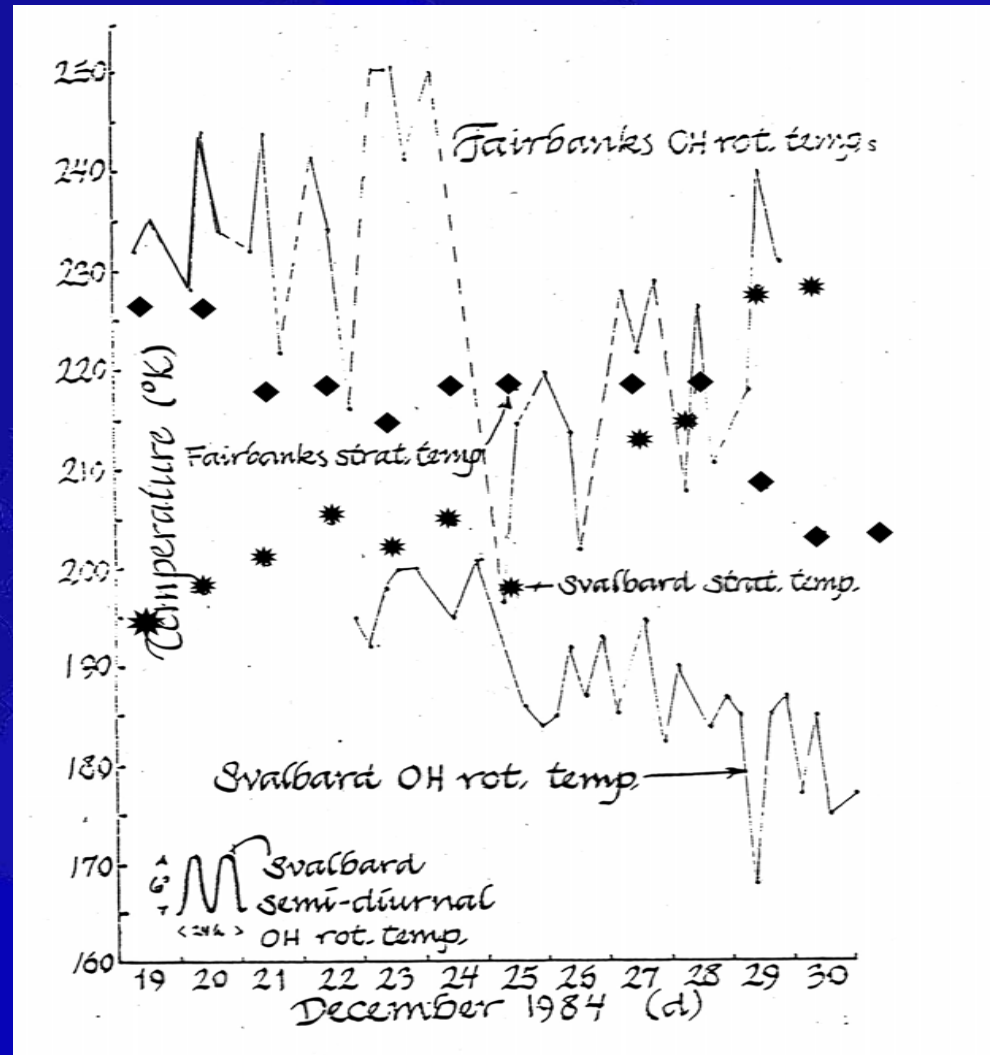
OH and O₂ Airglow

- Polar airglow emissions from the 85 & 100 km altitude regions.
- Temperature measured from relative emission line intensities.



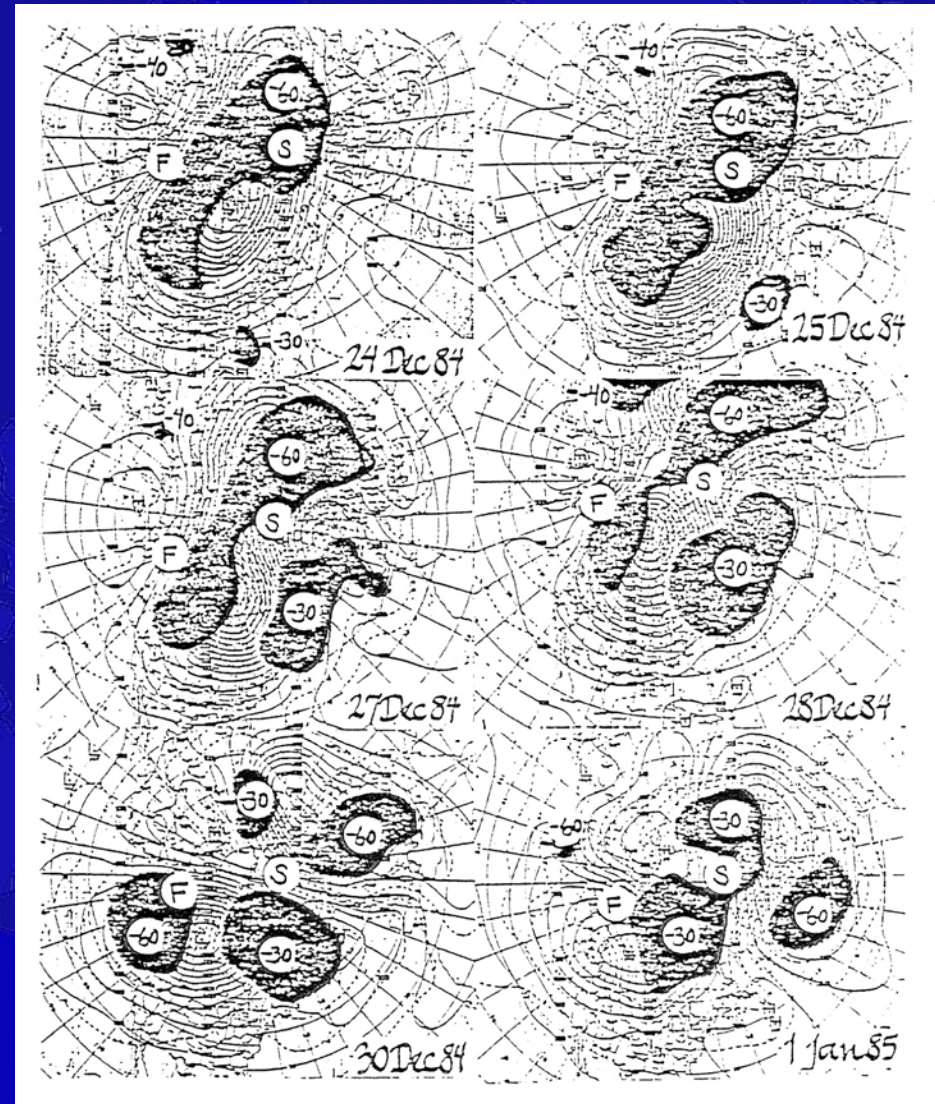
OH and O₂ Airglow

- Stratospheric warmings are associated with mesospheric cooling.
- Cooling occurs simultaneously over polar region.
- Stratwarm is regional



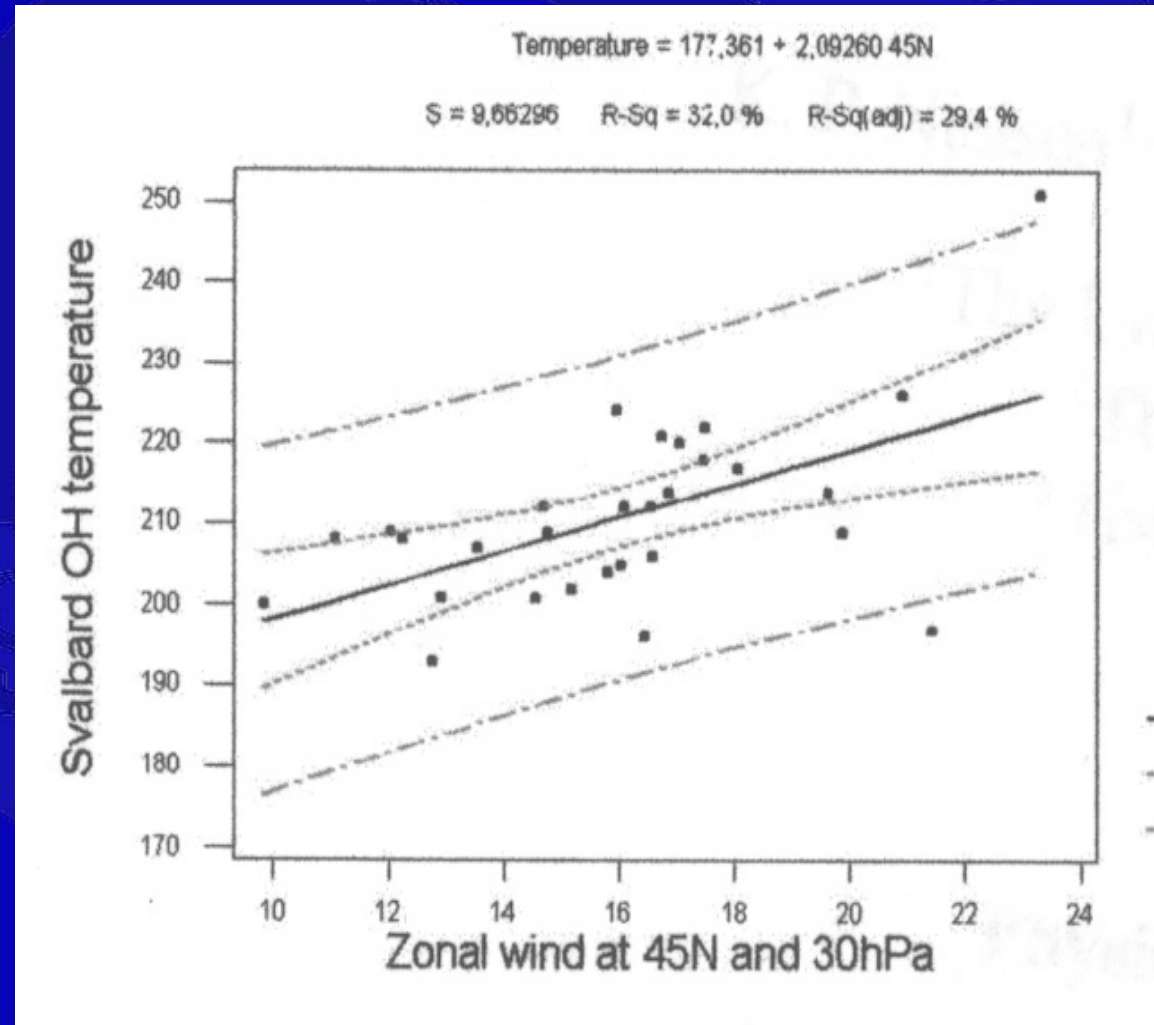
OH and O₂ Airglow

- Stratospheric warmings are associated with mesospheric cooling.
- Cooling occurs simultaneously over polar region.
- Stratwarm is regional.
- Note that small, warm (-30°) region circulates into polar region and breaks up cold polar stratosphere.



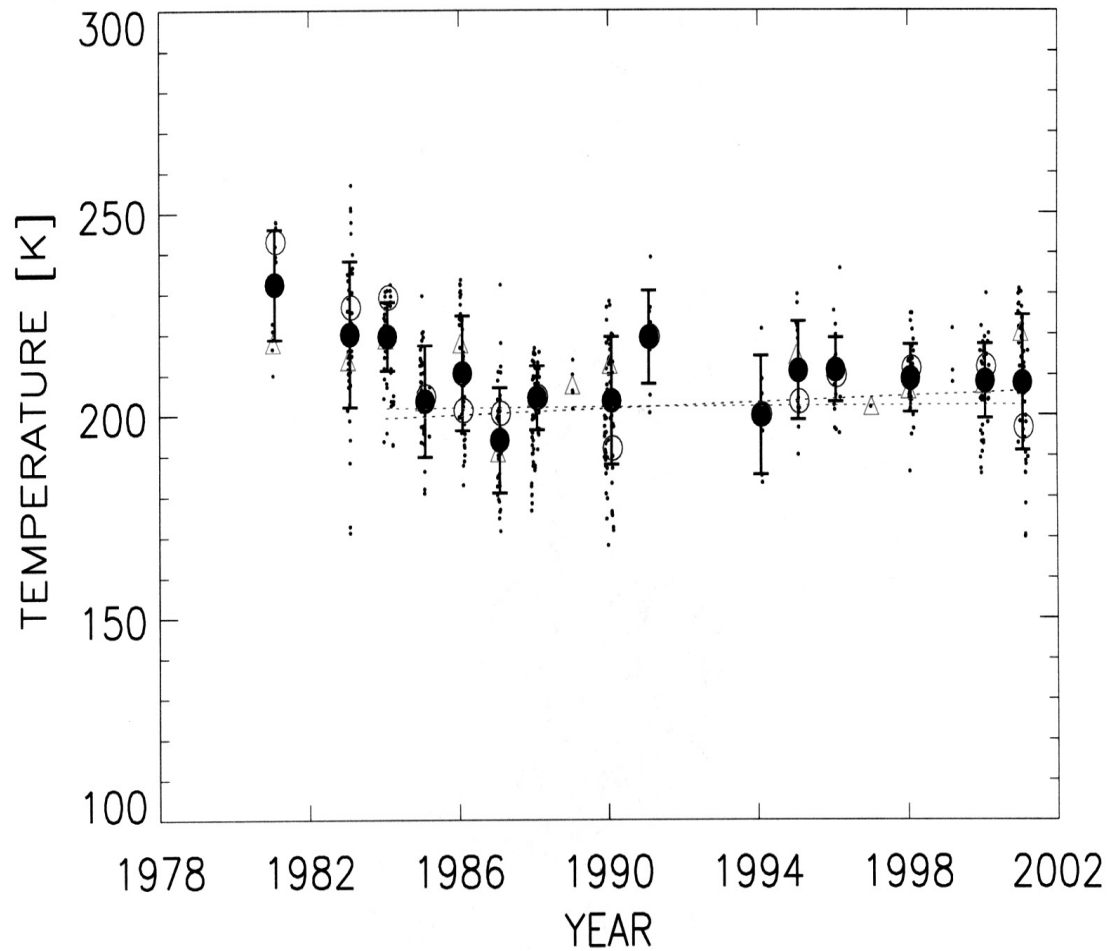
OH and O₂ Airglow

- Large variations in mesopause temperature are correlated best with the zonal wind at 30hPa near 45° N lat.



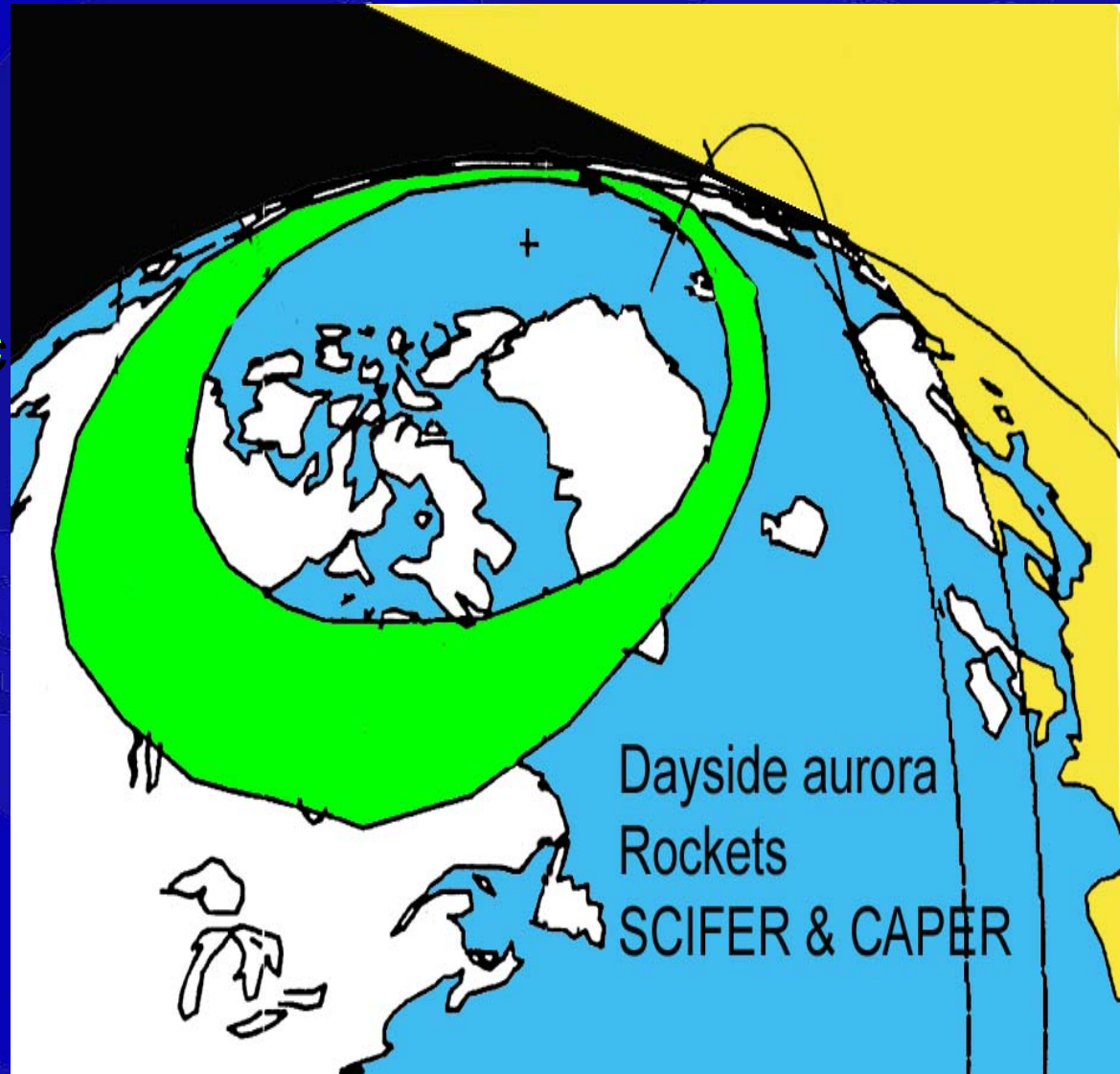
OH and O₂ Airglow

- Large variations in mesopause temperature are correlated best with the zonal wind at 30hPa near 45° N lat.
- 20 year record shows little change in mesopause temperature at 78° N Lat.



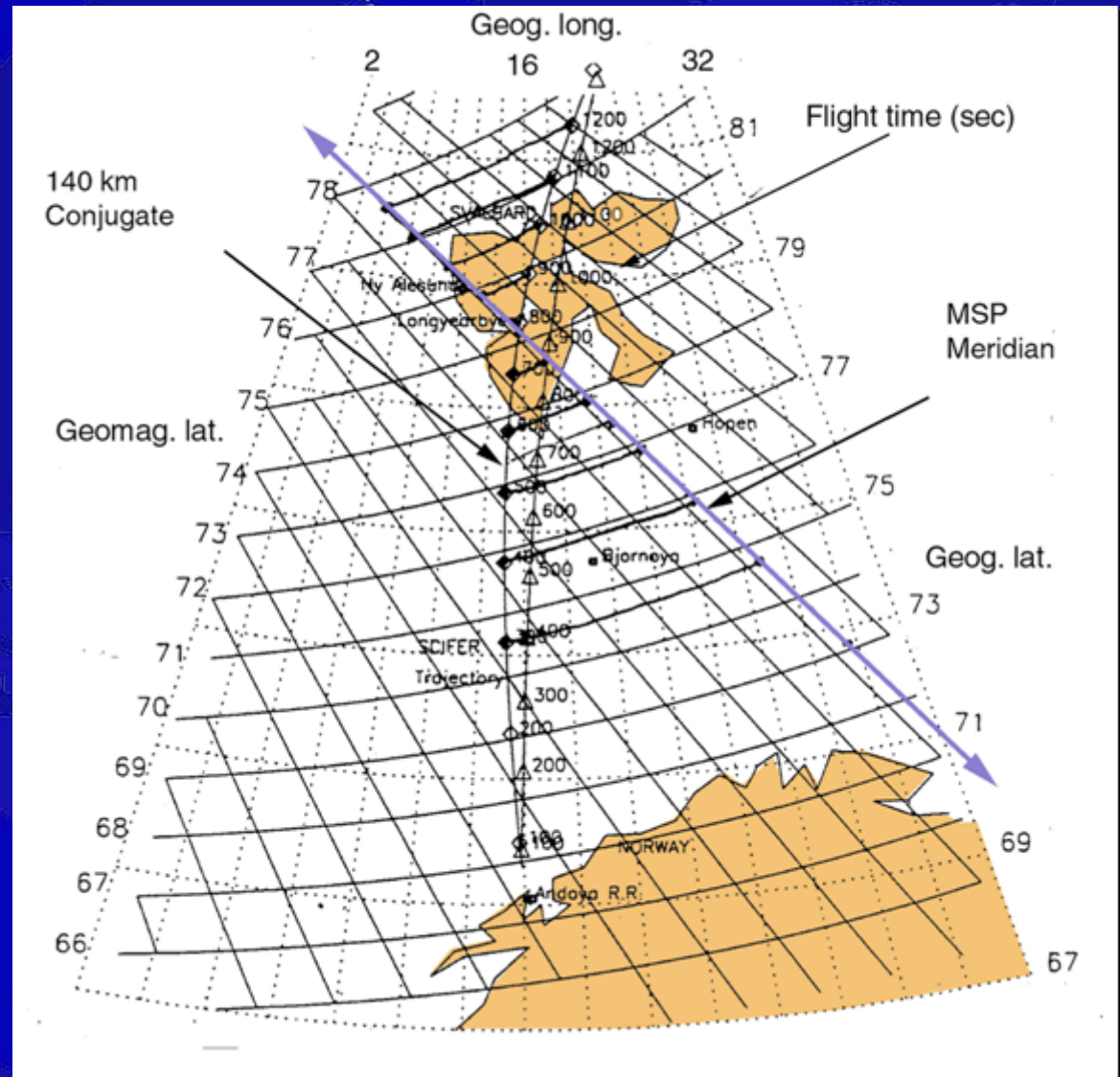
“SCIFER” Rocket Observations

- Rocket borne observations coordinated with ground-based optical and magnetic data.
- Launched from Andoya 06:24:48, January 25, 1995.
- Apogee 1452 km over Svalbard near 75° MLat. 10 MLT.

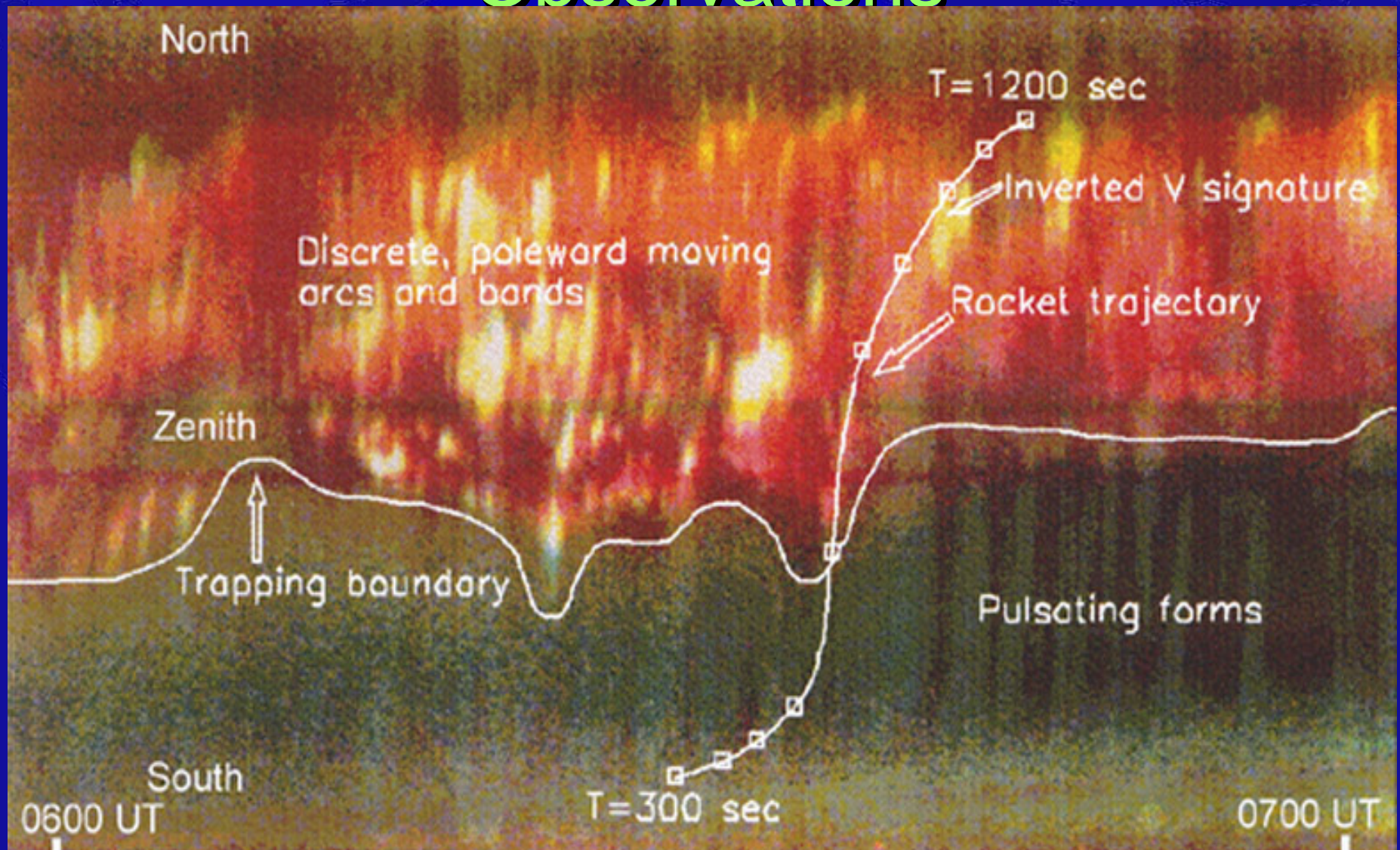


SCIFER Trajectory

- Trajectory was directly over Svalbard.
- 140 km magnetic conjugates below trajectory are linked to MSP along constant geomagnetic L shells.

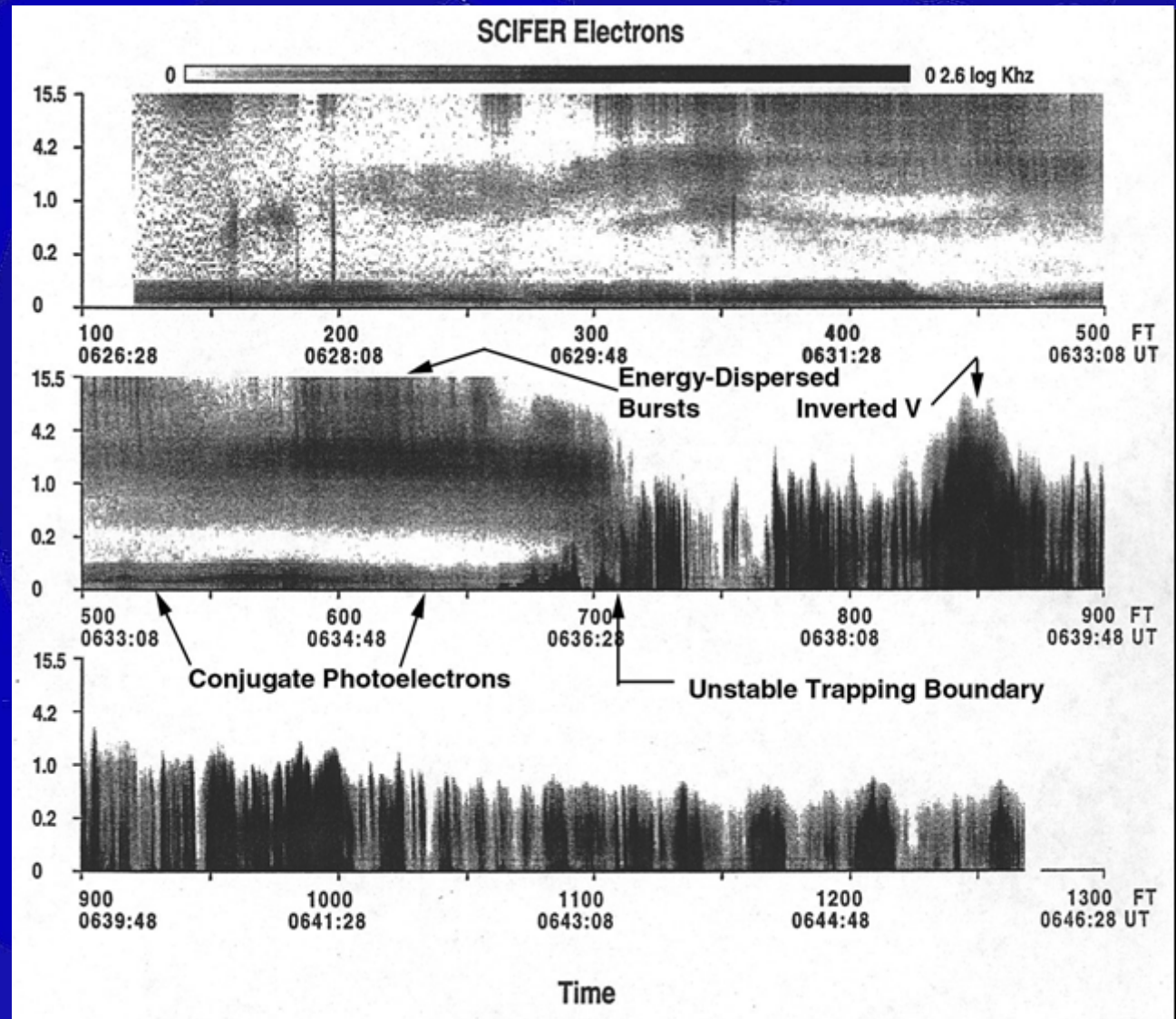


SCIFER Optical Auroral Observations



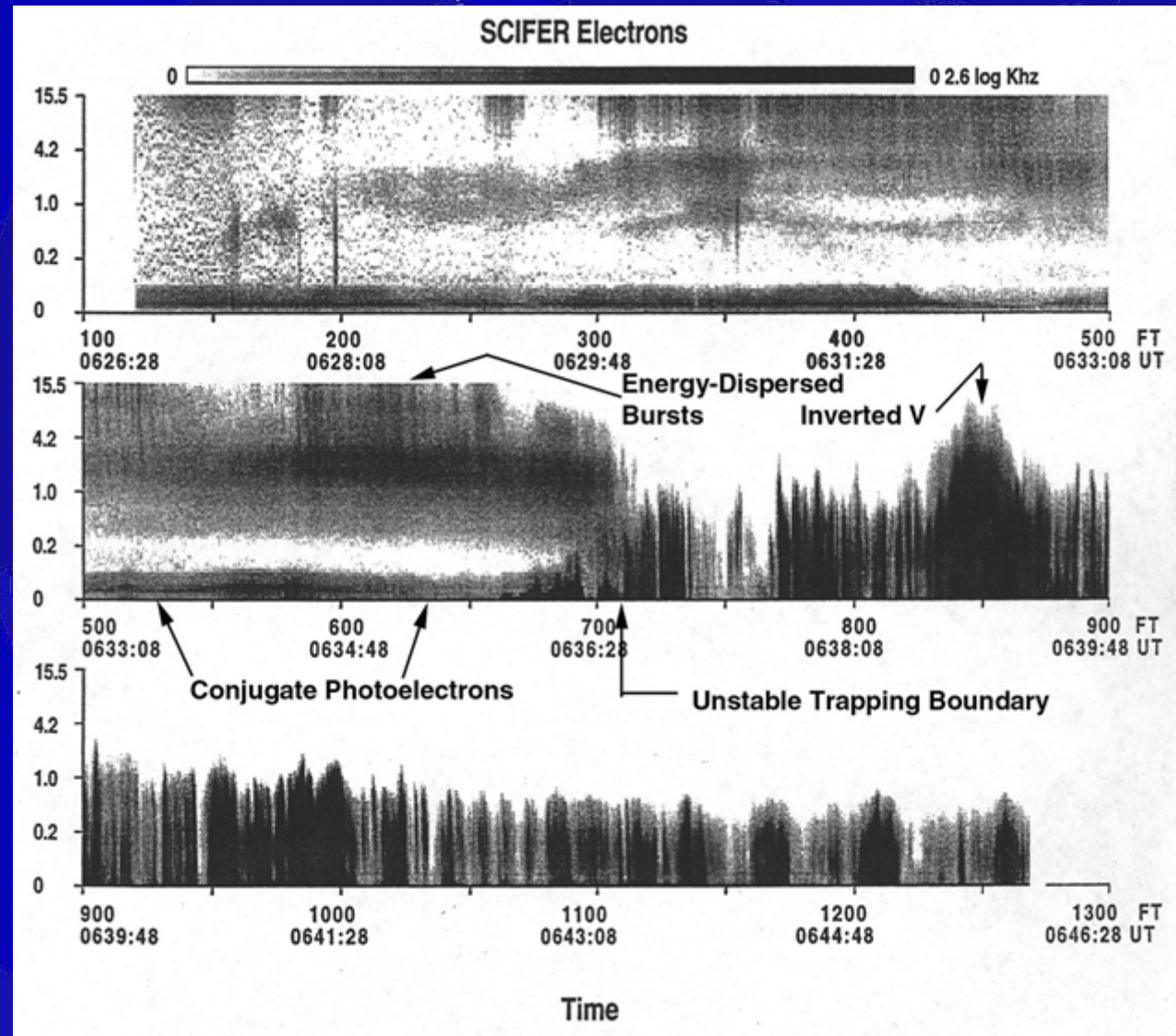
SCIFER Energetic Electron Flux

- Objective of the study is to identify the ionospheric signatures of the various particle populations.



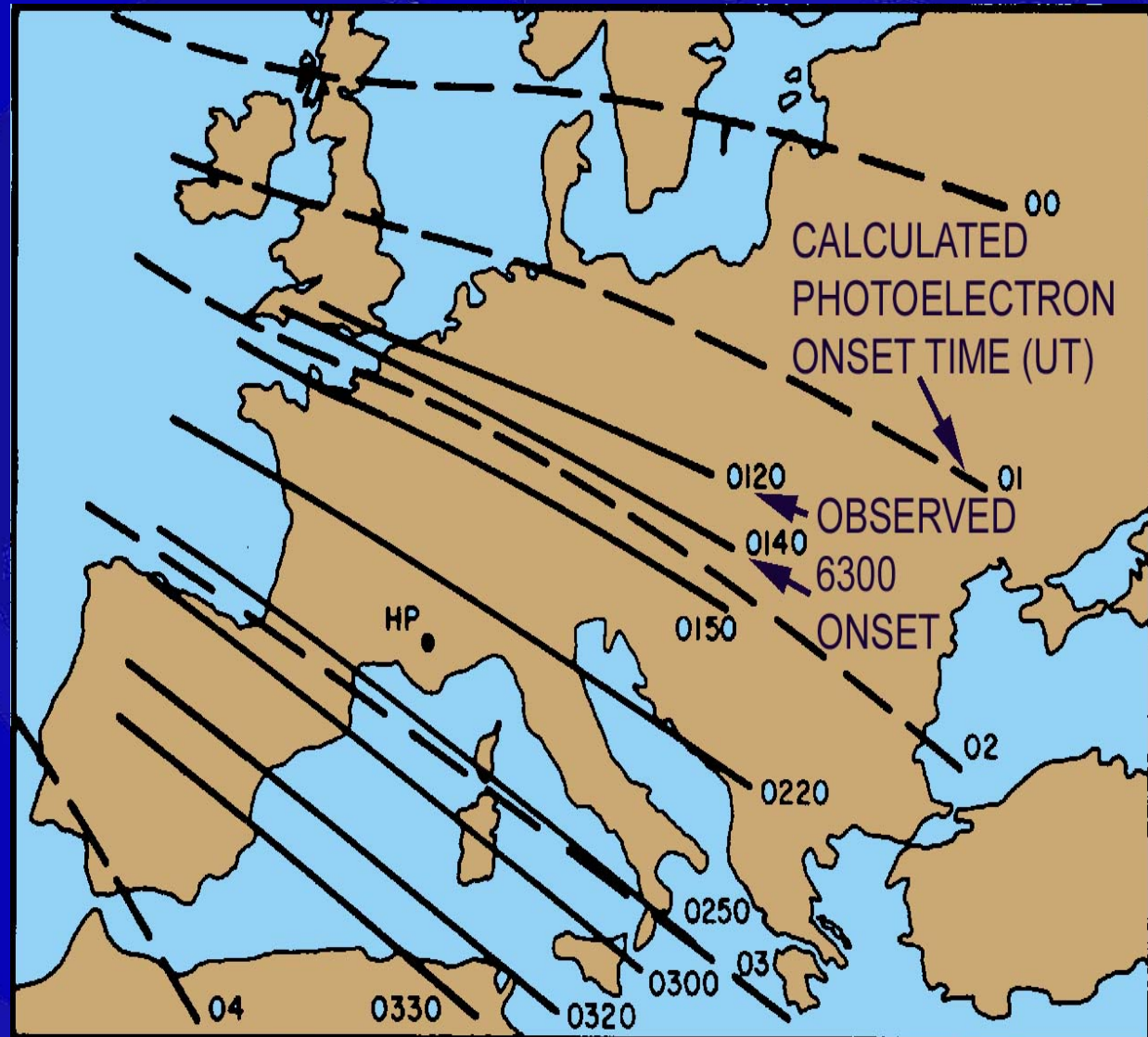
Photoelectron Poleward Boundary

- SCIFER flight at 1450 km over dayside aurora.
- Electron trapping boundary at 720 sec flight time.
- Magnetic zenith at LYR ($L=15$).
- Isotropic electron flux < 100 eV equatorward from boundary



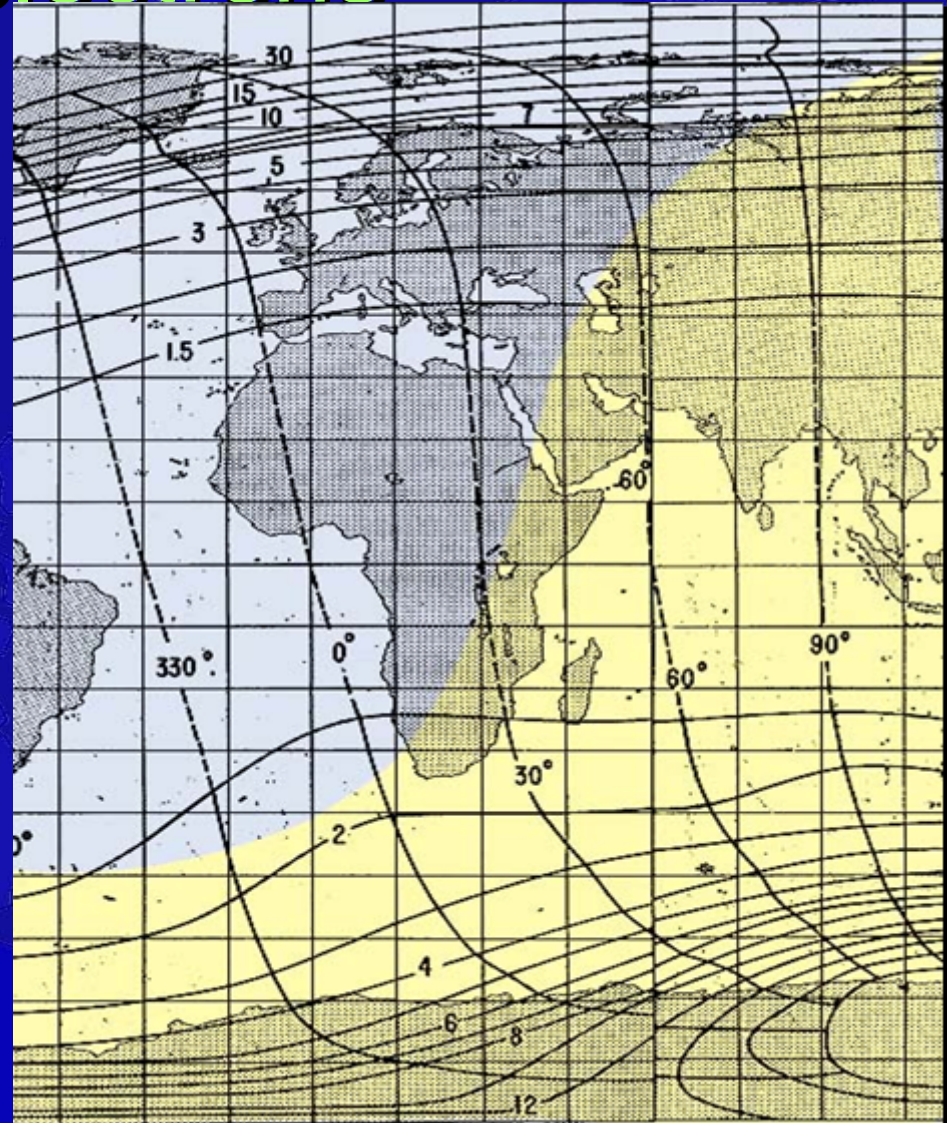
Predawn Enhancement 6300Å Airglow

- Observations from France by Barbier
- England by Roger Smith
- I. S. Radar Community
- Alaska and Oslo by C. Deehr
- Kiruna attempt with G. Gustavson



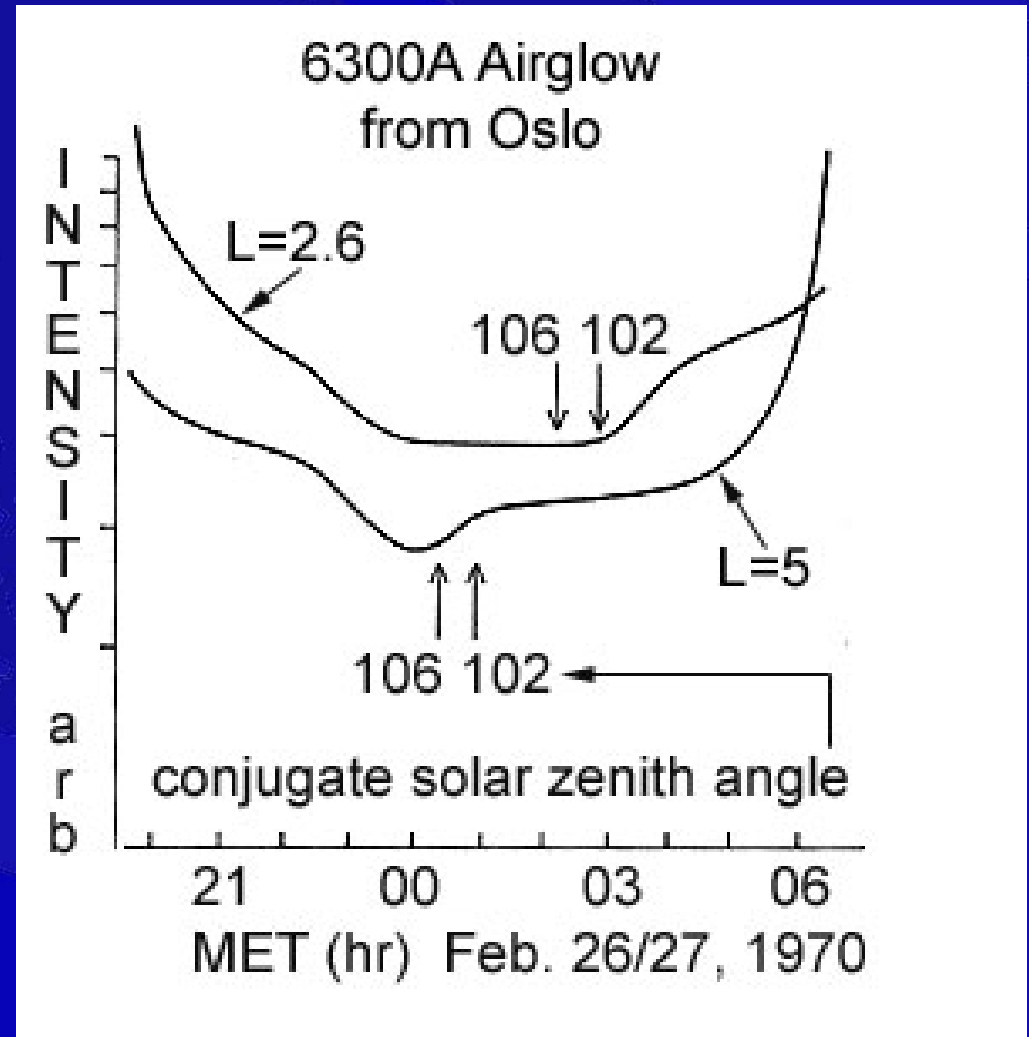
Magnetic Conjugate Photoelectrons

- This is a map of the extent of sunlit atmosphere during northern winter at 0200 UT. (astronomical twilight)
- The tilt of the geomagnetic field relative to the equatorial plane is such that the southern conjugate region is sunlit well before dawn over Europe.



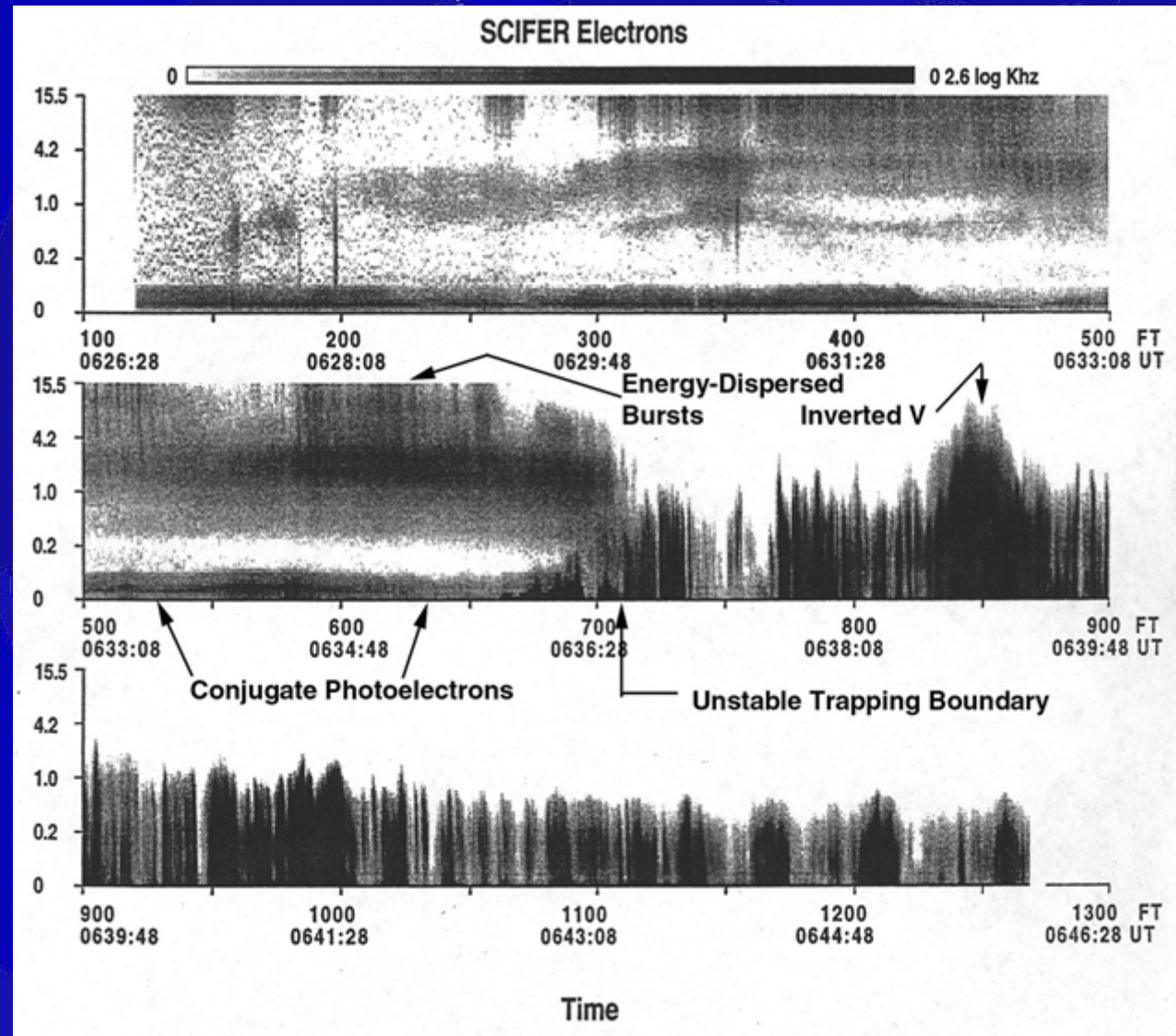
Conjugate Photoelectrons from Oslo

- Birefringent photometer from the roof of the Chemistry Building at University of Oslo.
- Increase in 6300 Å airglow seen to coincide with the conjugate solar zenith angles 90-106 for $L = 2.6$ (SSW) and $L = 5$ (NNW).



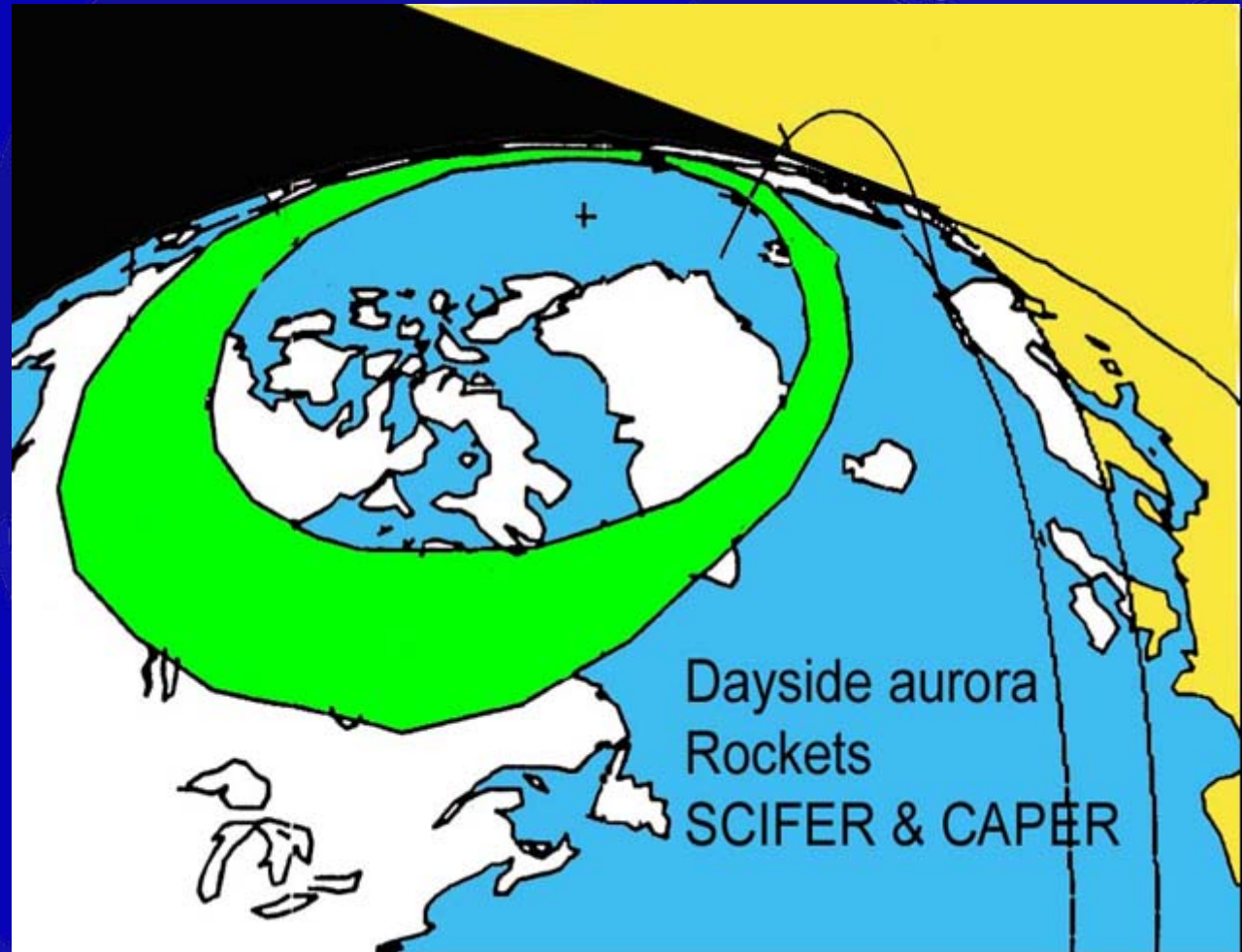
Photoelectron Poleward Boundary

- SCIFER flight at 1450 km over dayside aurora.
- Electron trapping boundary at 720 sec flight time.
- Magnetic zenith at LYR ($L=15$).
- Isotropic electron flux < 100 eV equatorward from boundary



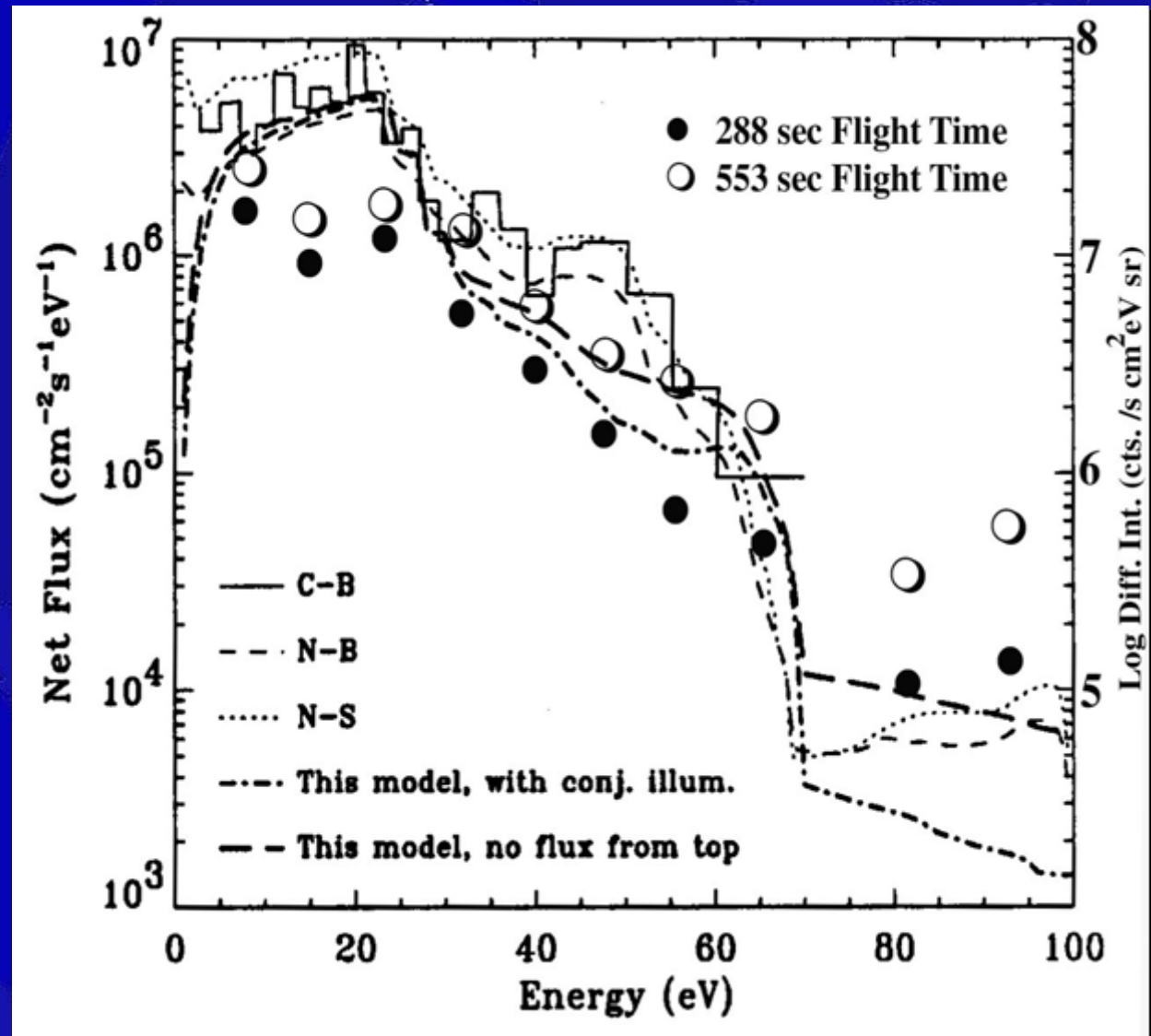
Photoelectron Poleward Boundary

- Expected limit was $L=4$.
- Difficult to detect 100 to 200 R of 6300 Å emission near the auroral oval at $L=5-6$.
- SCIFER and CAPER rockets launched over the dayside aurora ($L=6$ to 30).



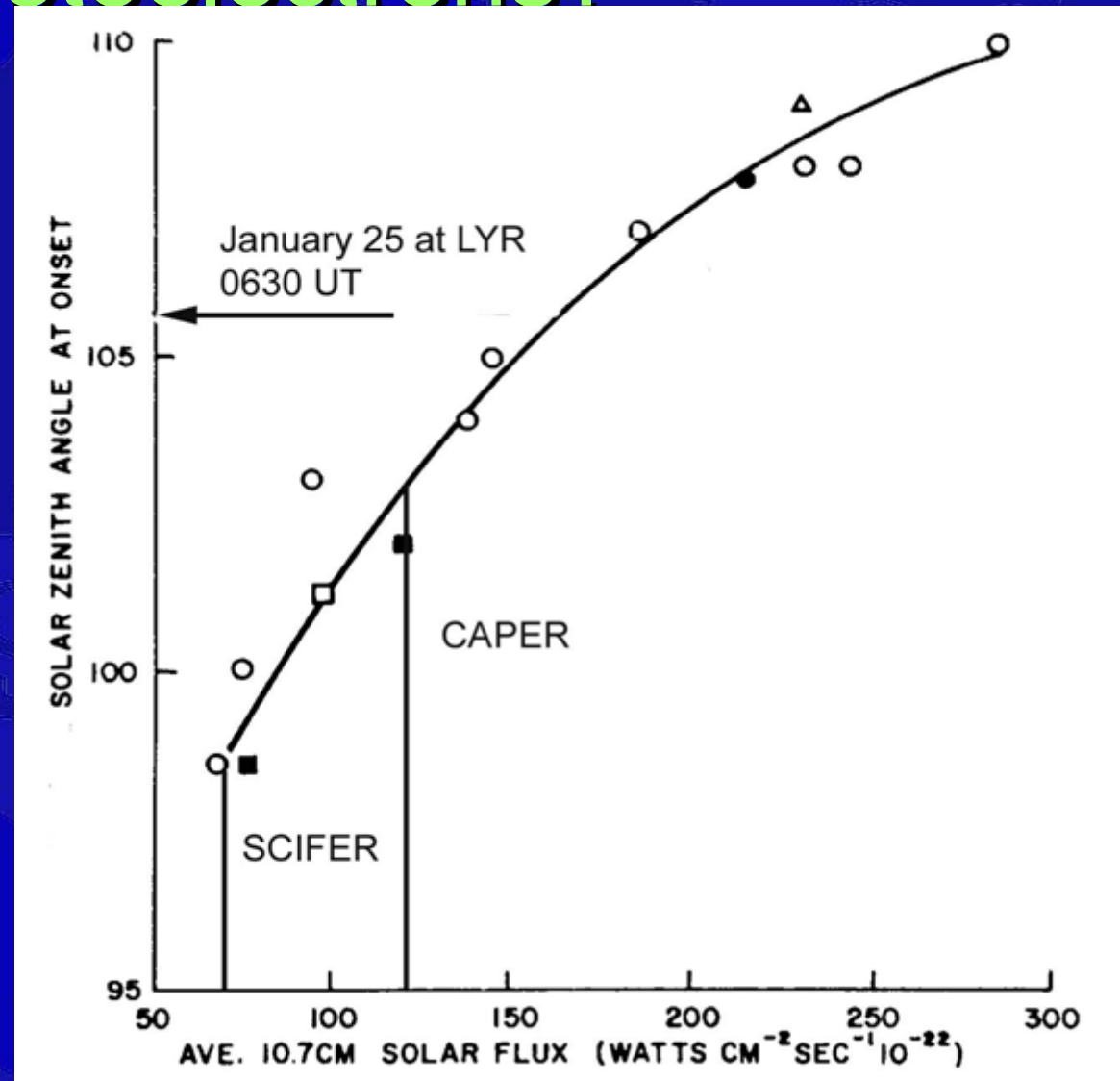
Photoelectron Energy Spectrum

- Theoretical photoelectron spectrum by G. Khasanov shows detail due to structure in solar EUV flux.
- SCIFER observations indicate photoelectrons.



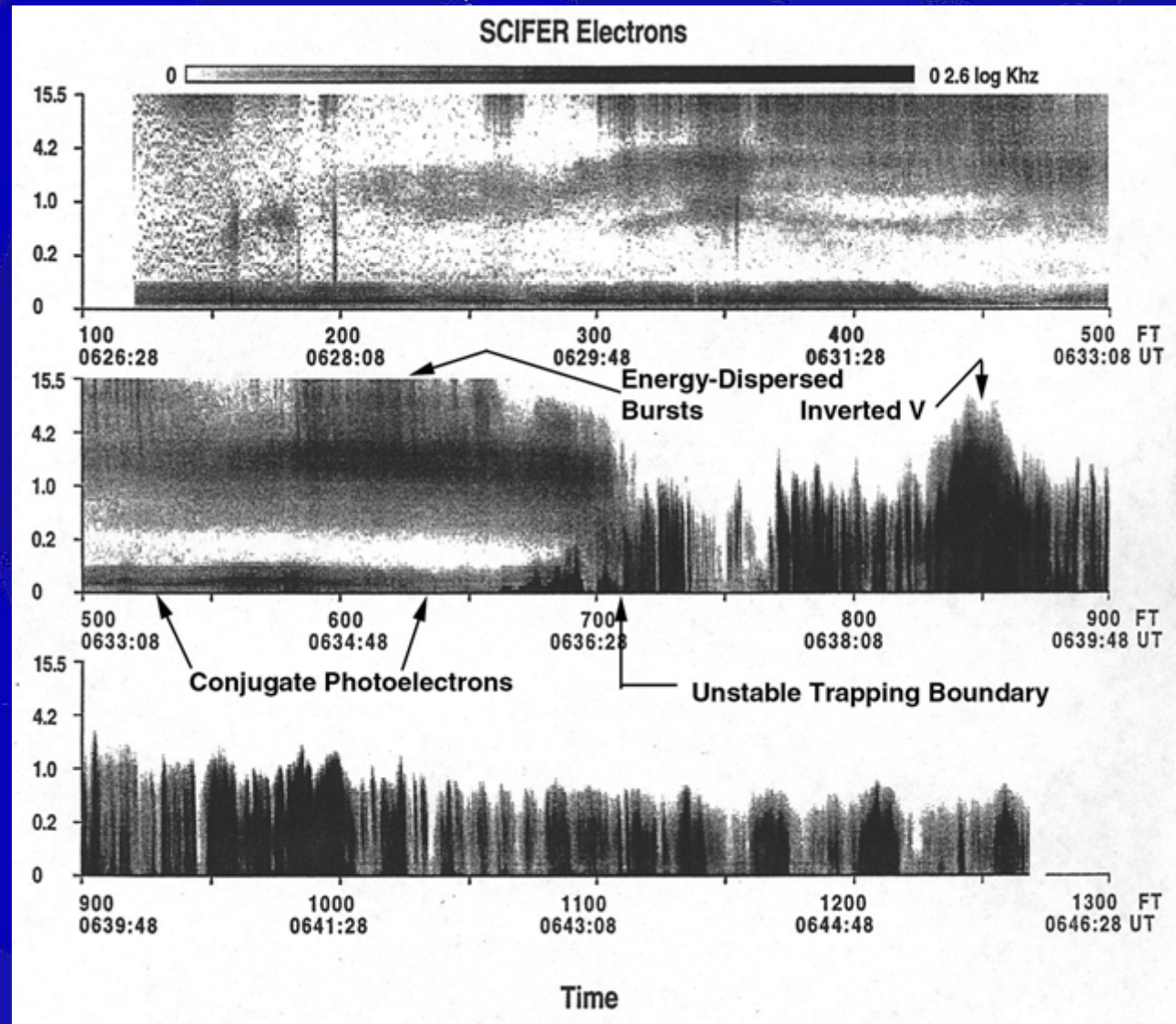
Local or Conjugate Photoelectrons?

- Earliest local production of photoelectrons is dependent on solar EUV flux.
- Proxy for EUV is 10.7 cm flux.
- Solar EUV during SCIFER and CAPER below that required to produce local photoelectrons at 106° sza.



SCIFER Energetic Electron Flux

- Objective of the study is to identify the ionospheric signatures of the various particle populations.
- 0-80 eV are photoelectrons from conjugate region.



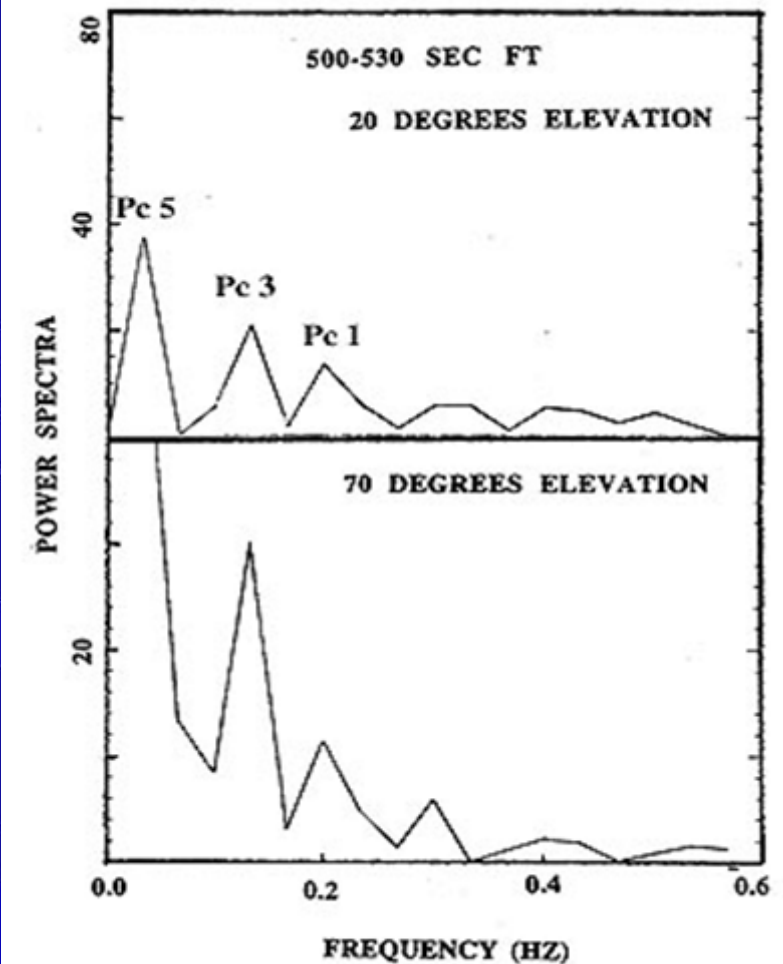
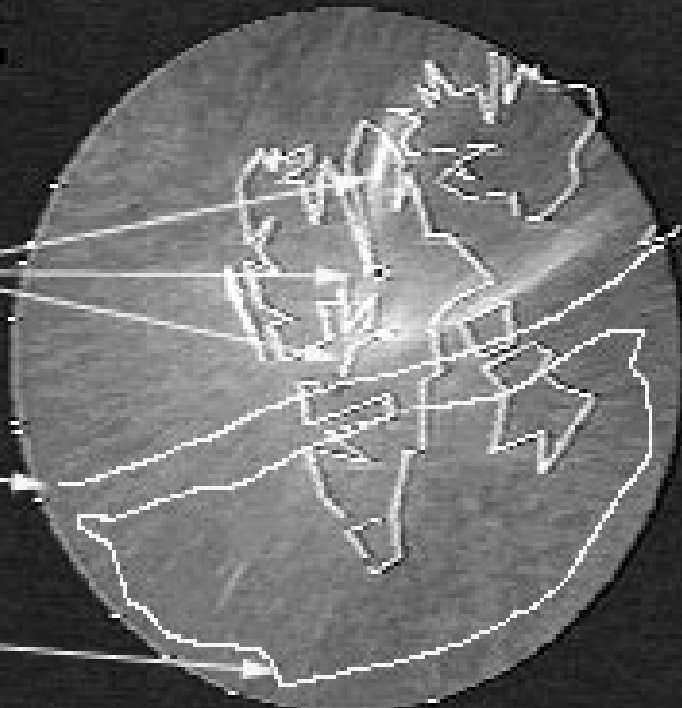
Southern Sky Brightness Pulsations

1995/01/25
06:38:49 UT
alt 120 km

Discrete
Auroral
Bands

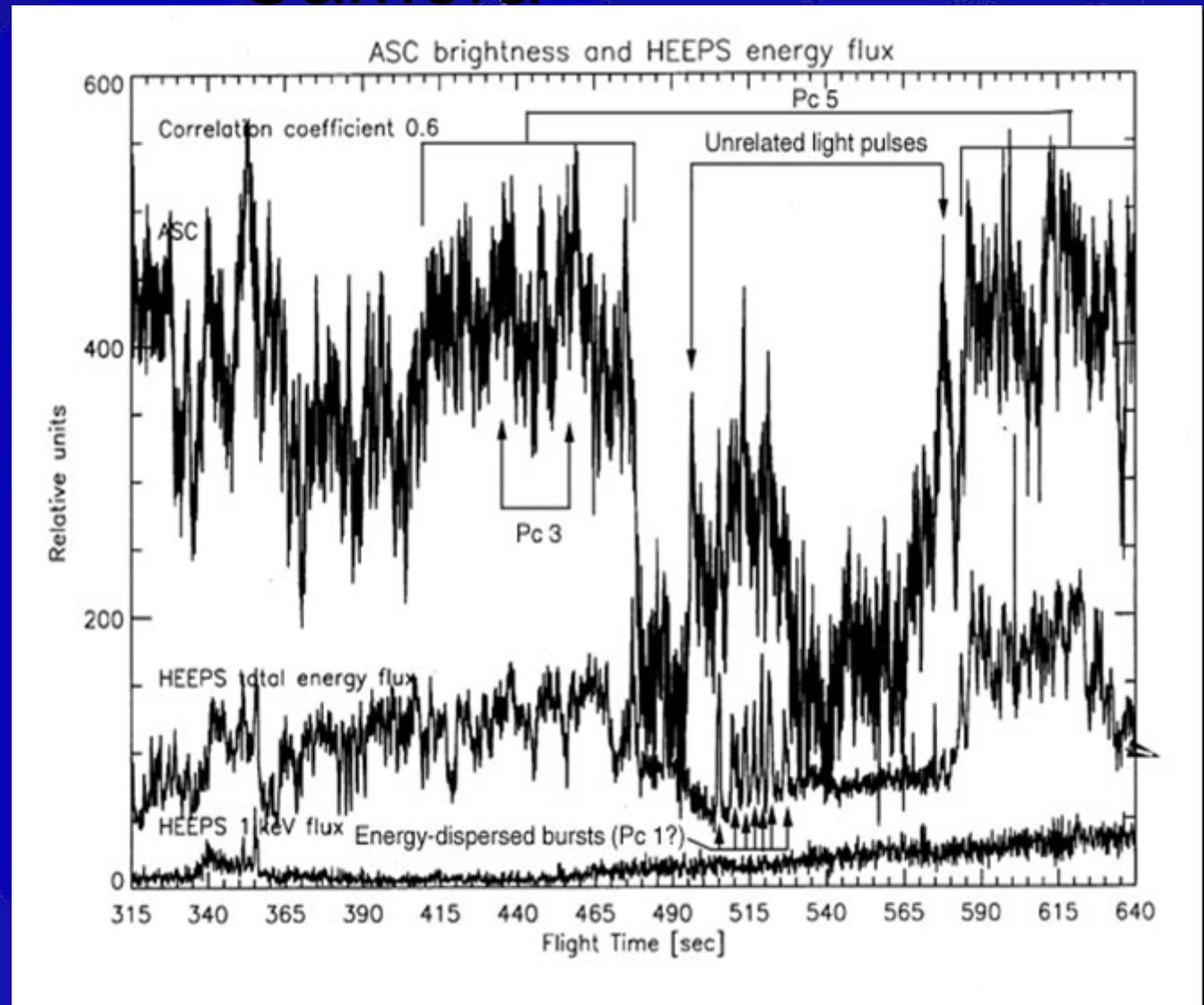
Trapping
Boundary

Pulsating
Aurora



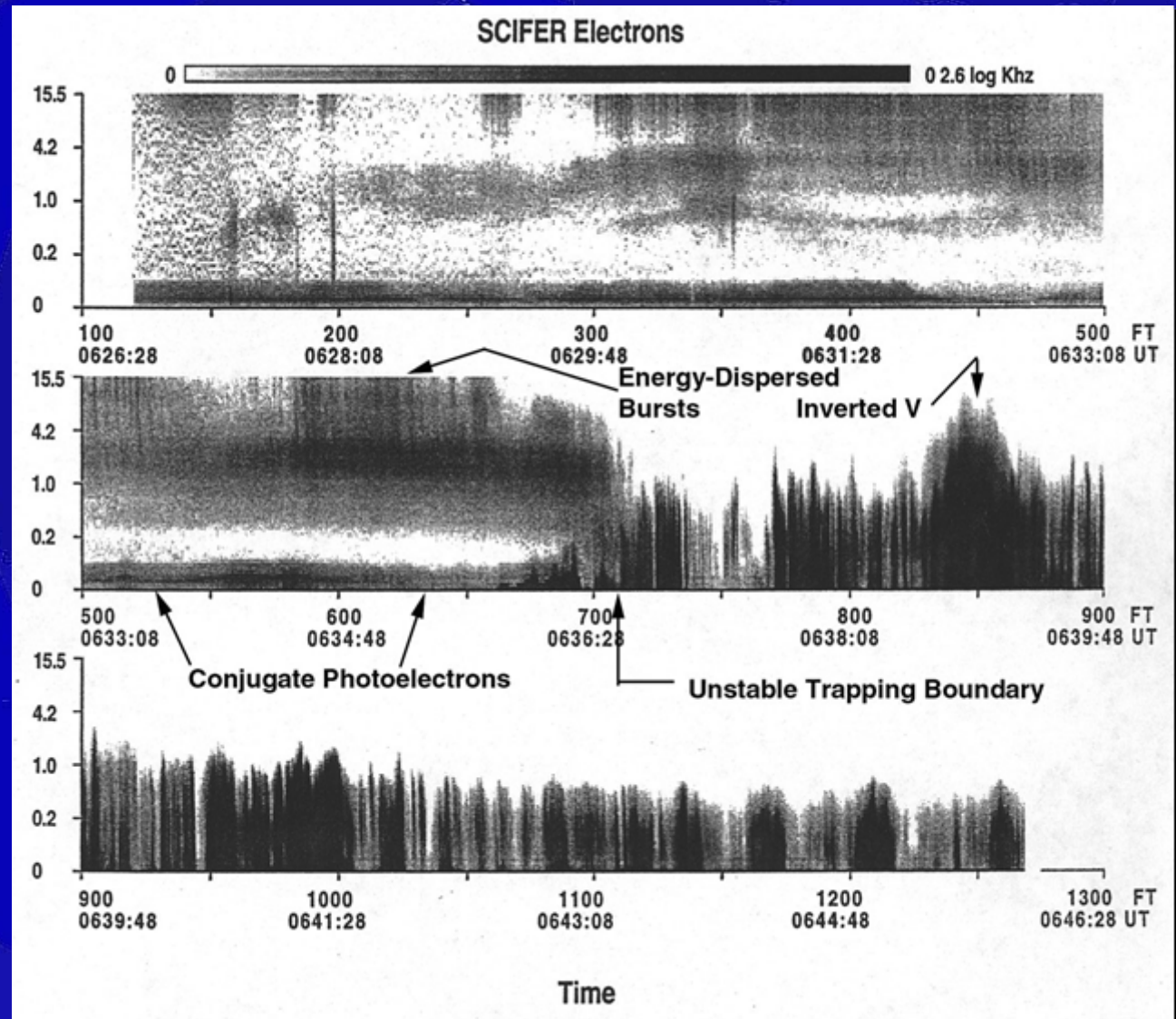
Particle Energy Flux & All-Sky Camera

- Total correlation coeff. = 0.6
- Variations with periods of magnetic pulsations Pc 1, 3, 5 are shown.
- There are two pulses that are unrelated.
- Pc 5 (180 s) and Pc 3 (43 s) correlate with 1-5 keV electron flux.



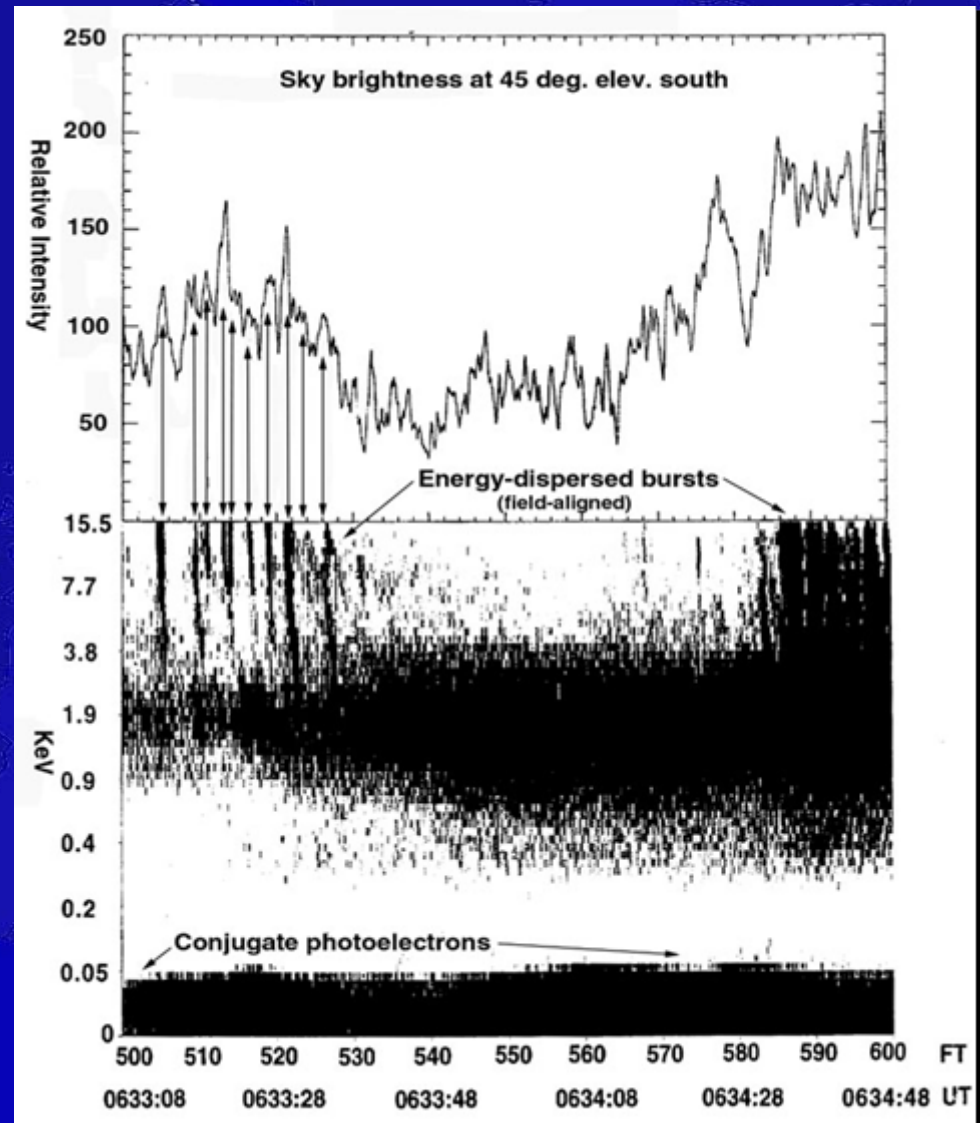
SCIFER Energetic Electron Flux

- Objective of the study is to identify the ionospheric signatures of the various particle populations.
- 0-80 eV (<700 sec) are conjugate photoelectrons.
- 1-5 keV (<700sec) are wave/particle interaction pulsations.



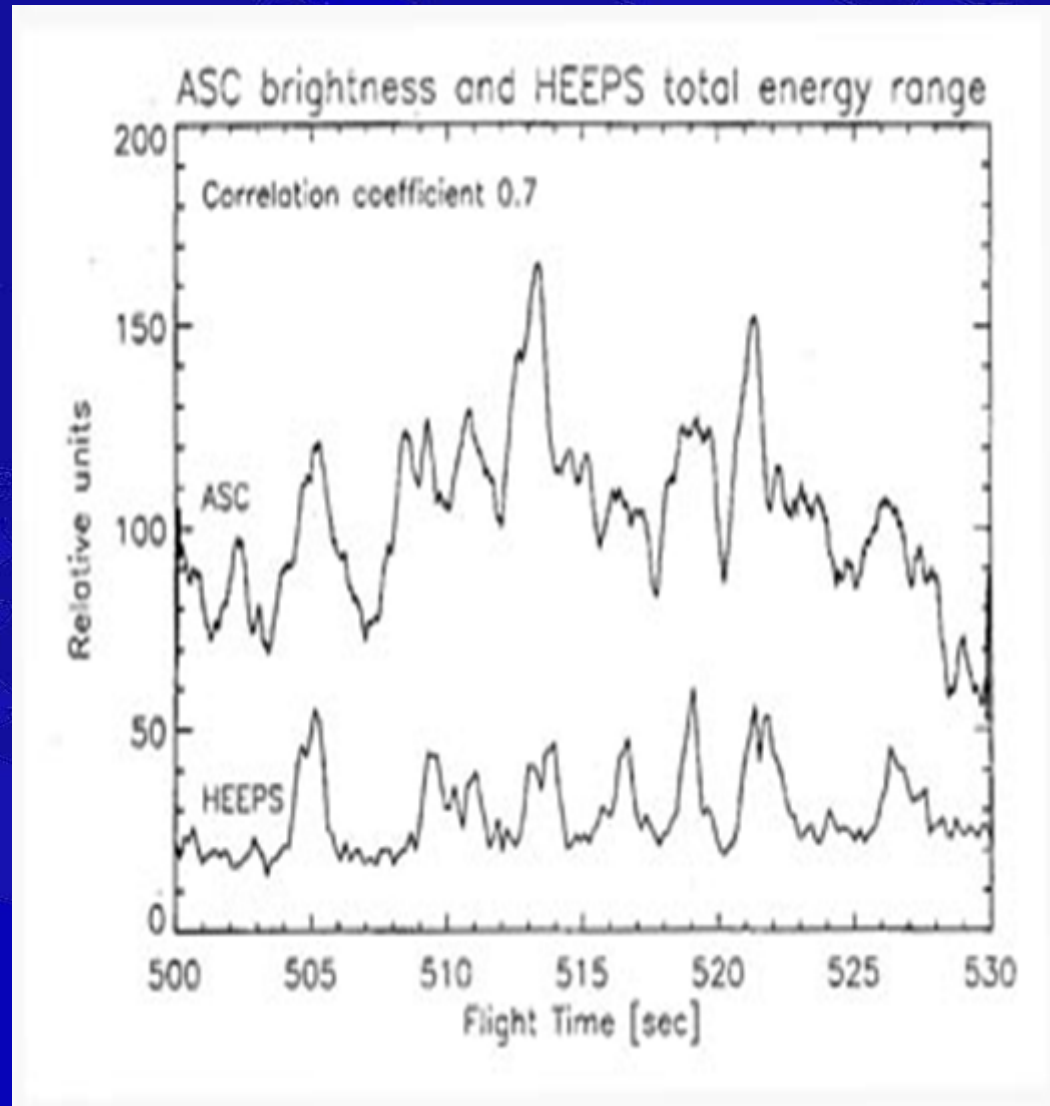
Energy-dispersed Bursts

- All-sky camera brightness pulses
- Energy dispersed from 1 to >15 keV.
- Dispersion indicates loss cone injection near equator.
- Bounce times = $n \times 1/2$ length of field line.
- Energy flux = $0.2 \text{ ergs/cm}^2\text{sec}$, implying most flux $> 15 \text{ keV}$.



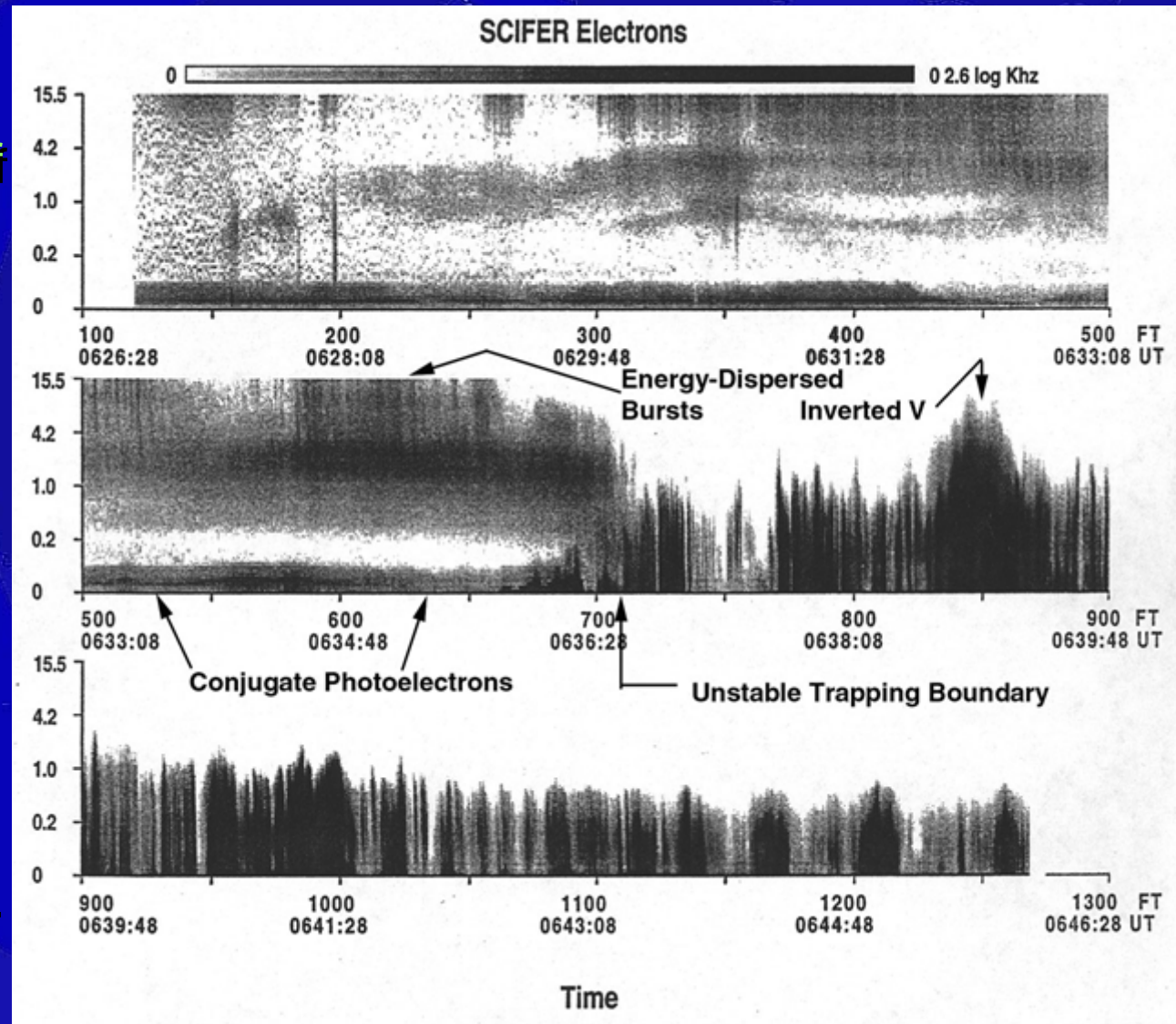
Particle Energy Flux & All-Sky Camera

- Sky brightness in the equatorward sky compared with simultaneous observations of energetic electron precipitation in the same region.
- Broad-band all-sky camera intensity pulses correlate with energy-dispersed bursts in the energetic electrons.
- Correlation coeff. = 0.7.
- There is no magnetometer data to confirm the relationship to Pc 1 pulsations

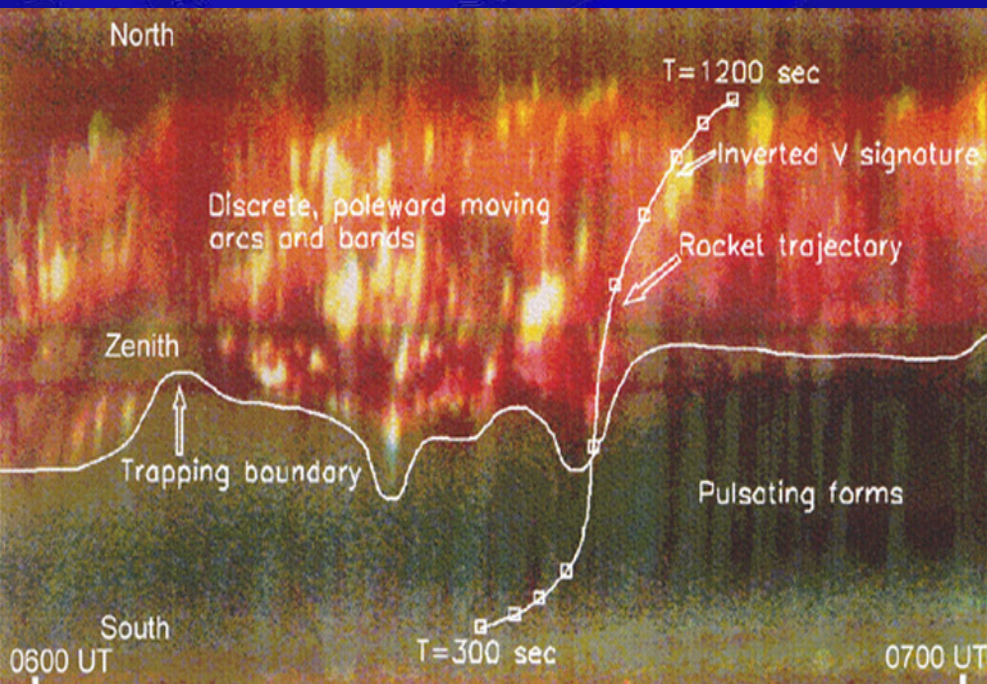


SCIFER Energetic Electron Flux

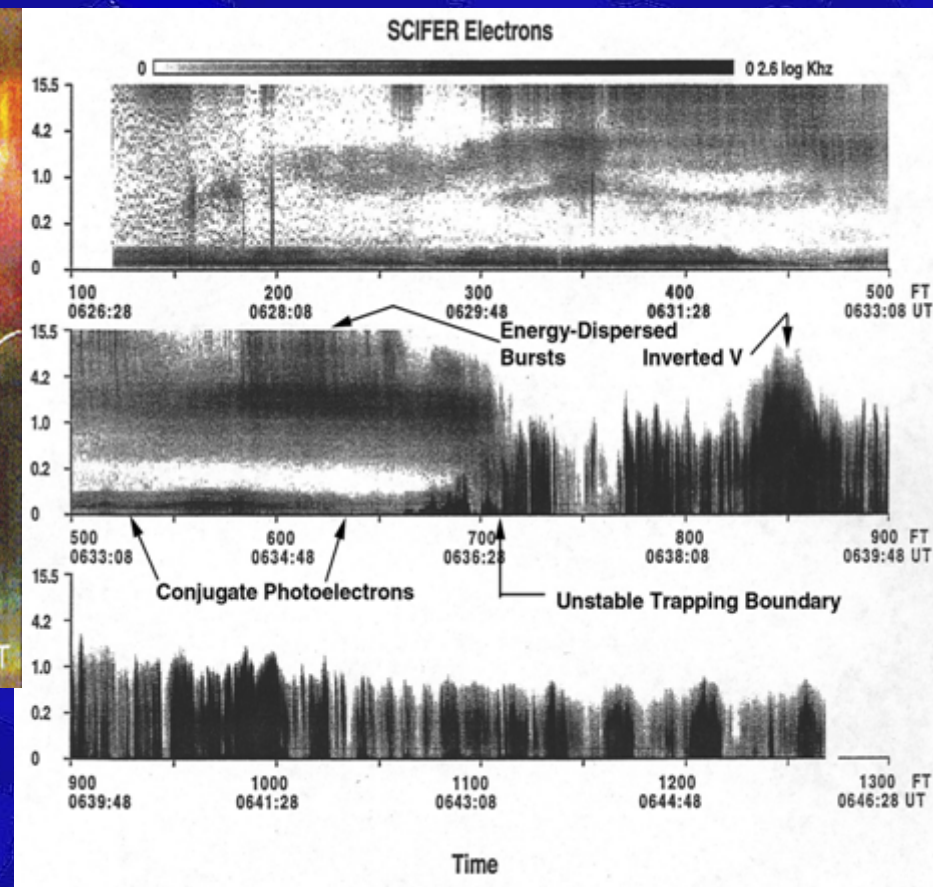
- Comparison of optical and particle data yields origin of particles.
- 0-80 eV are conjugate photoelectrons.
- 1-5 keV are wave/particle interaction along closed field line.
- >5 keV energy dispersed bursts from wave/particle interaction equator.



Poleward Discrete Arcs

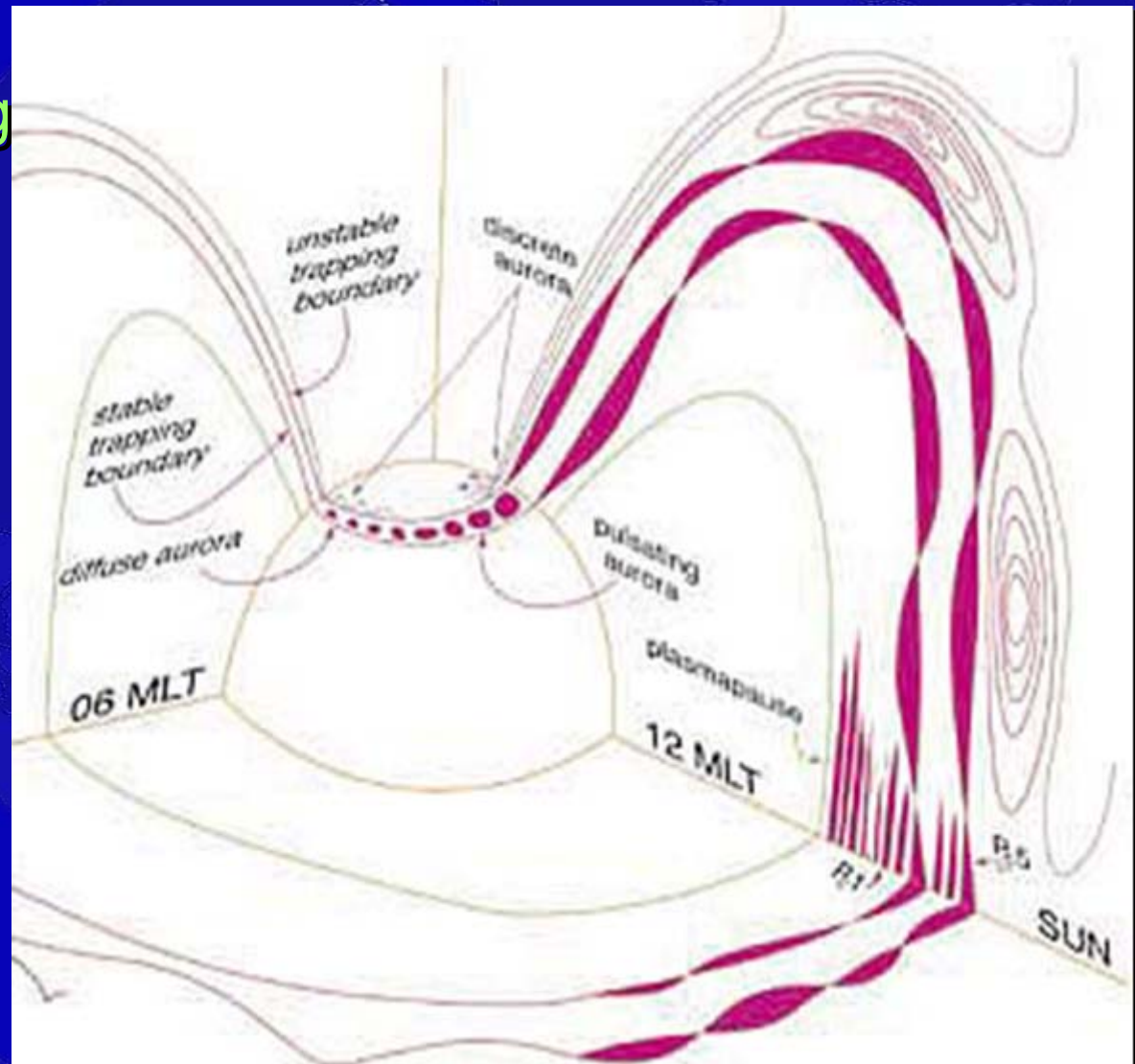


- Inverted V particle signature over discrete arcs.
- Peak $E > 1$ keV visible as arc on TV (~ 0.5 ergs/cm²sec).



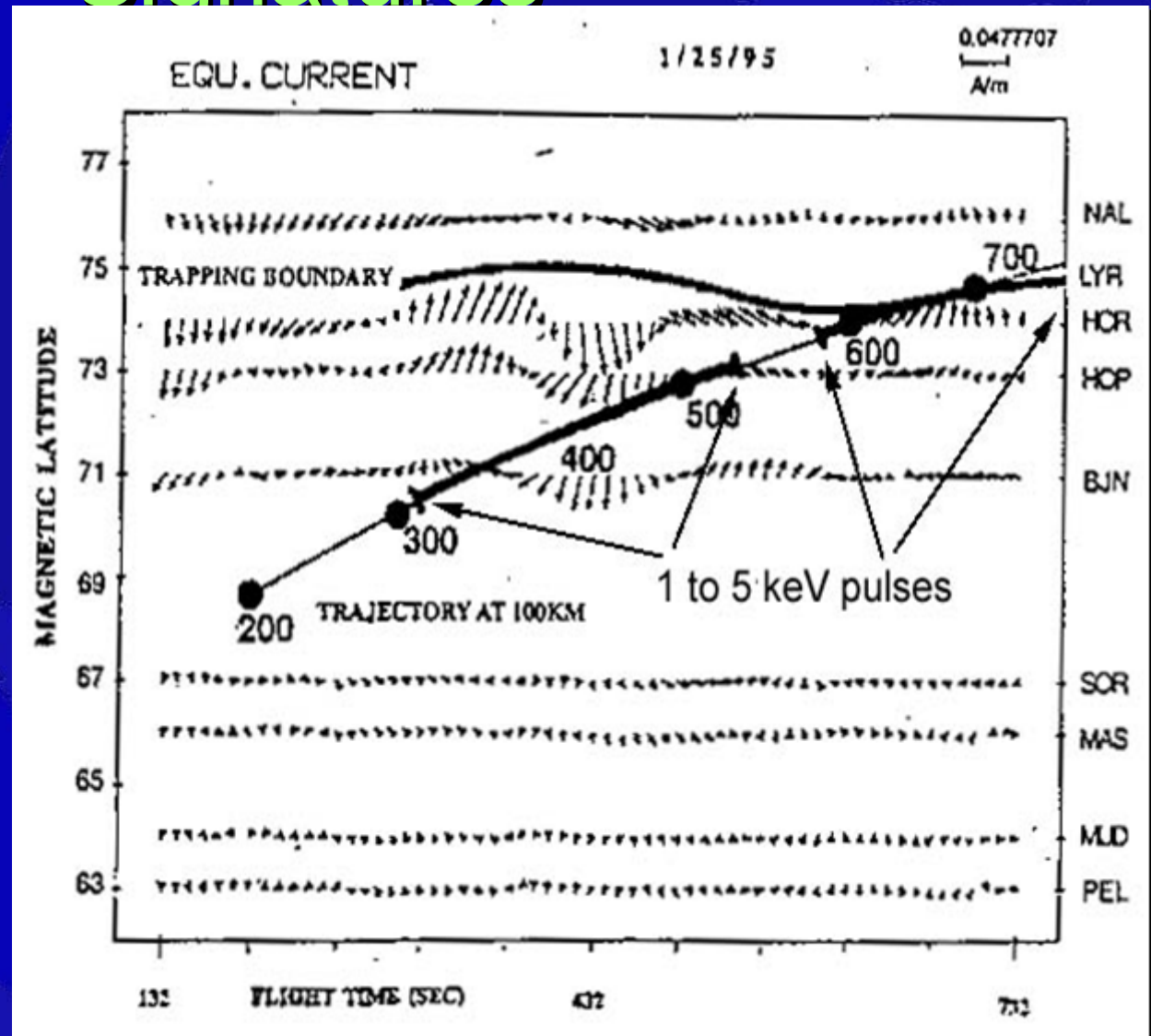
Magnetospheric Boundaries

- Discrete aurora poleward of trapping boundary.
- Wave/particle and merging processes produce pulsating aurora inside trapping boundary.



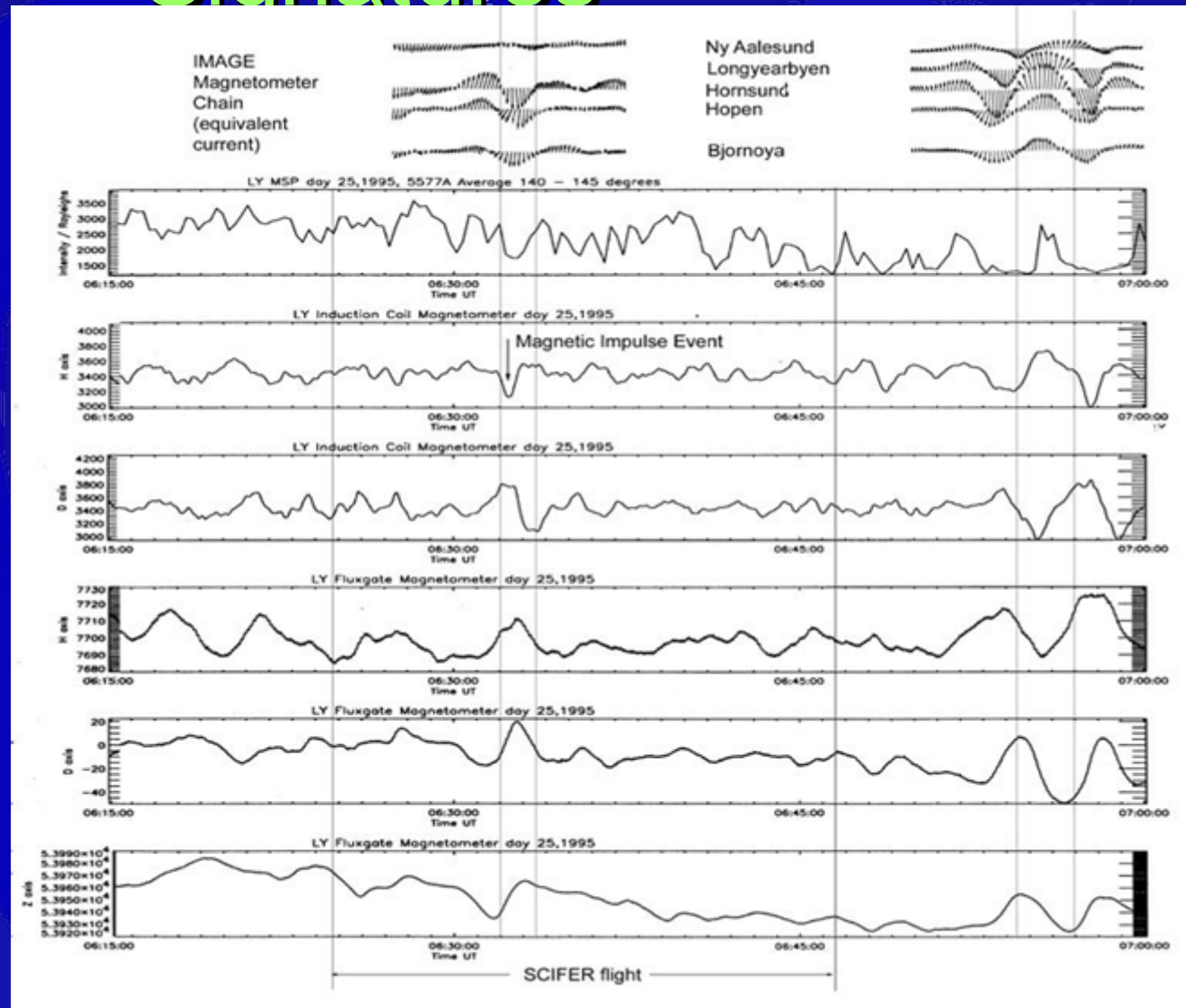
Geomagnetic Disturbance Signatures

- There were two pulses of 1-5 keV electrons during the flight.
- They corresponded to increase in brightness and Magnetic Convection Vortices.

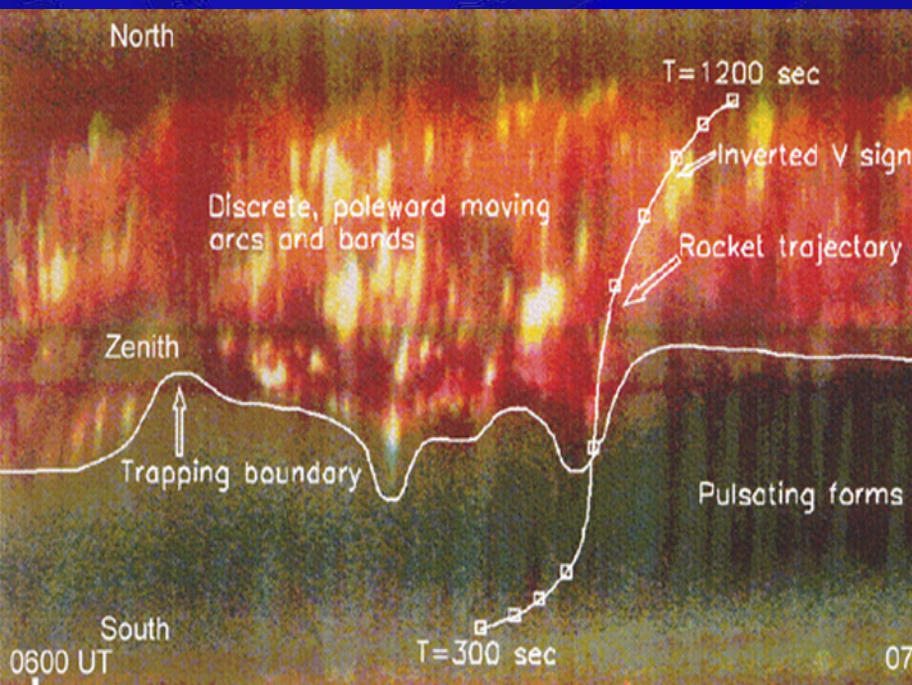


Geomagnetic Disturbance Signatures

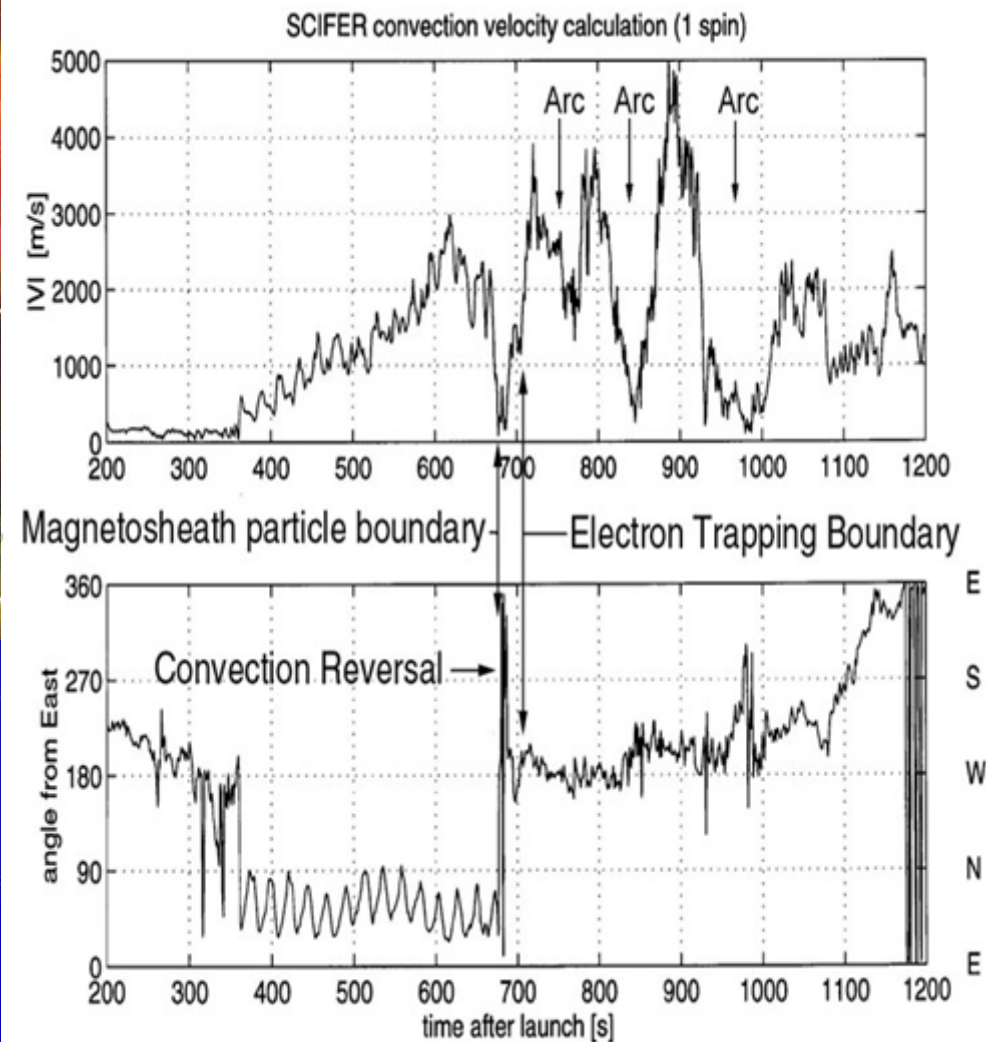
- The Pc 5 magnetic pulsations, the optical pulsations and the TCV are produced by the 1-5 keV electron pulses inside the trapping boundary.



Convection Velocity

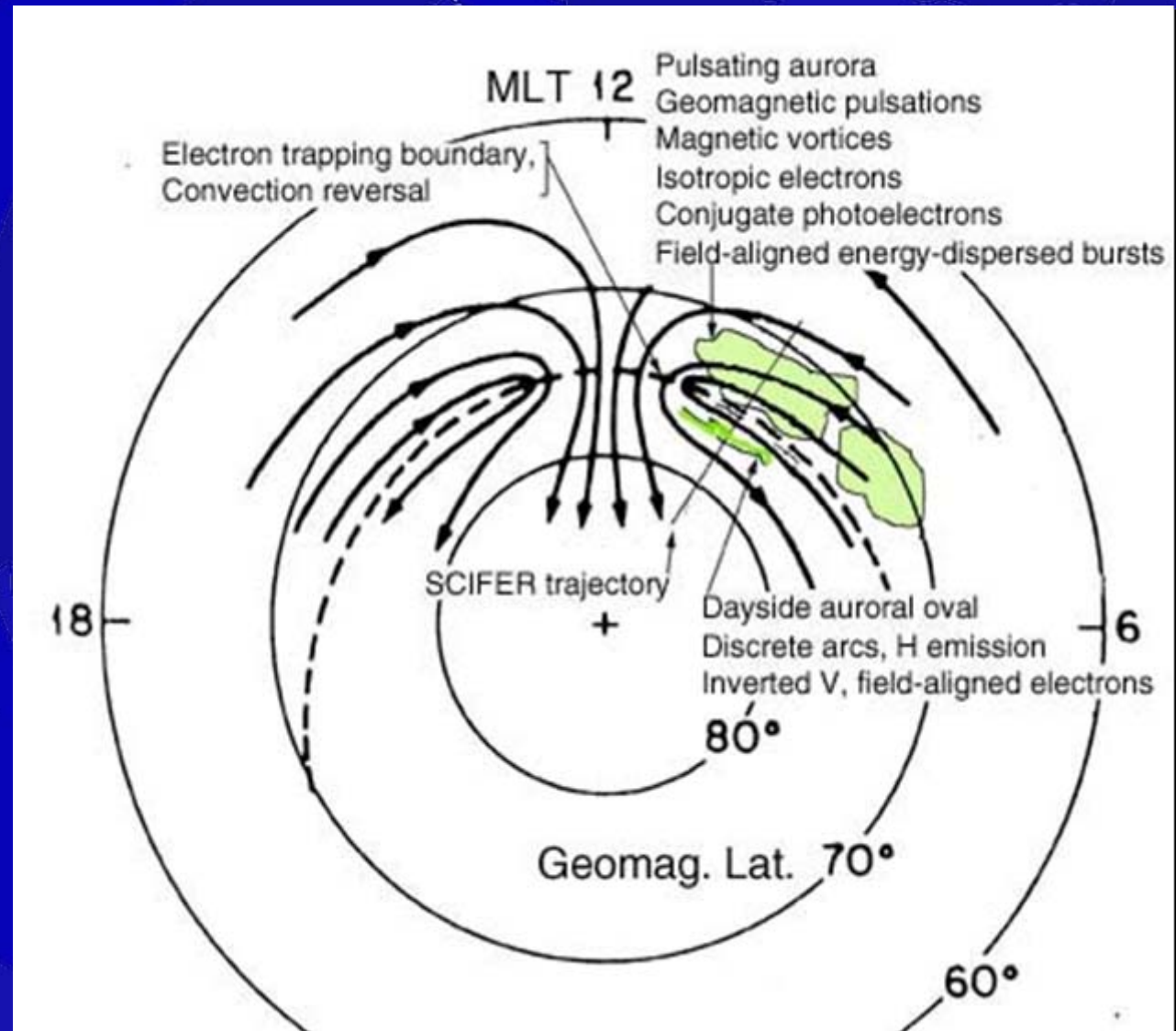


- Convection sunward inside trapping boundary.
- Anti-sunward poleward.
- Speed minimum inside arcs.



Relationship to Convection Pattern

- Midmorning.
- IMF $B_z < 0$.
- 40 keV trapping boundary coincident with convection reversal.

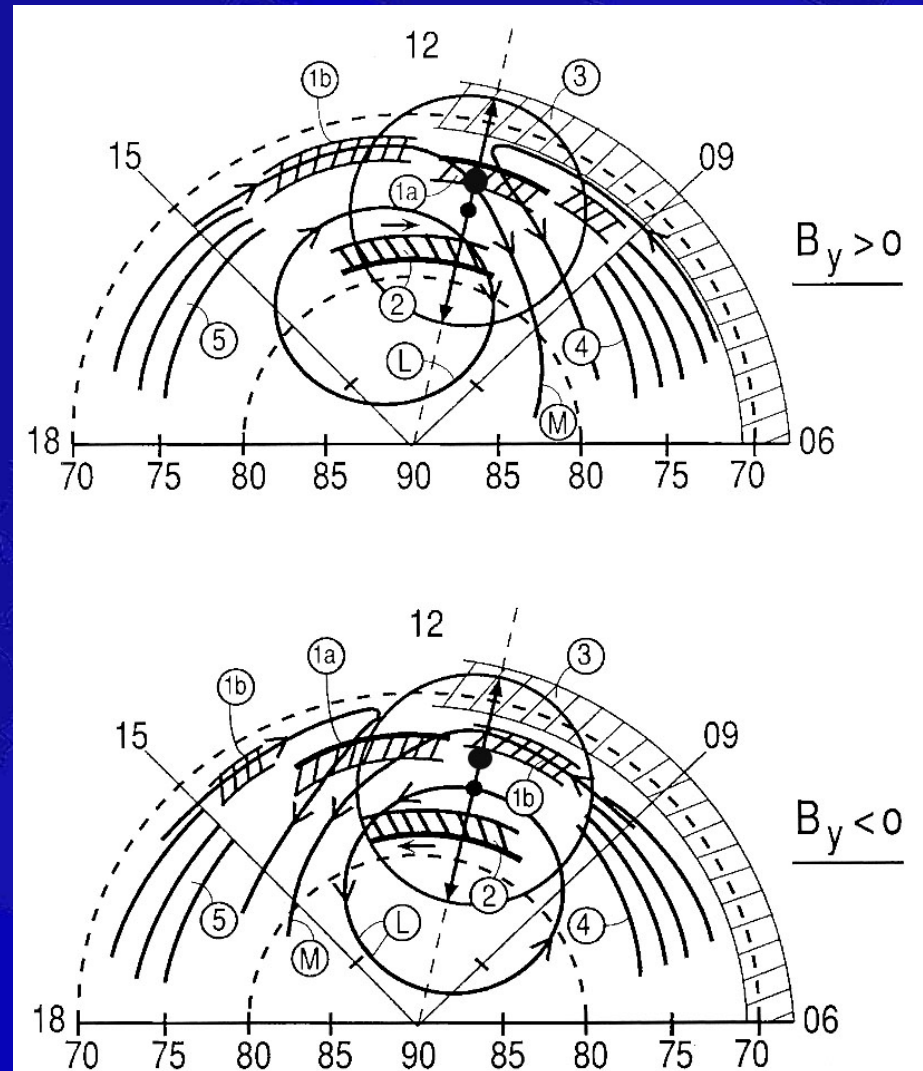


- IMF $B_z < 0$.
- IMF $B_y > 0$.
- PMAFs near 40.
- Ion dispersion observed.



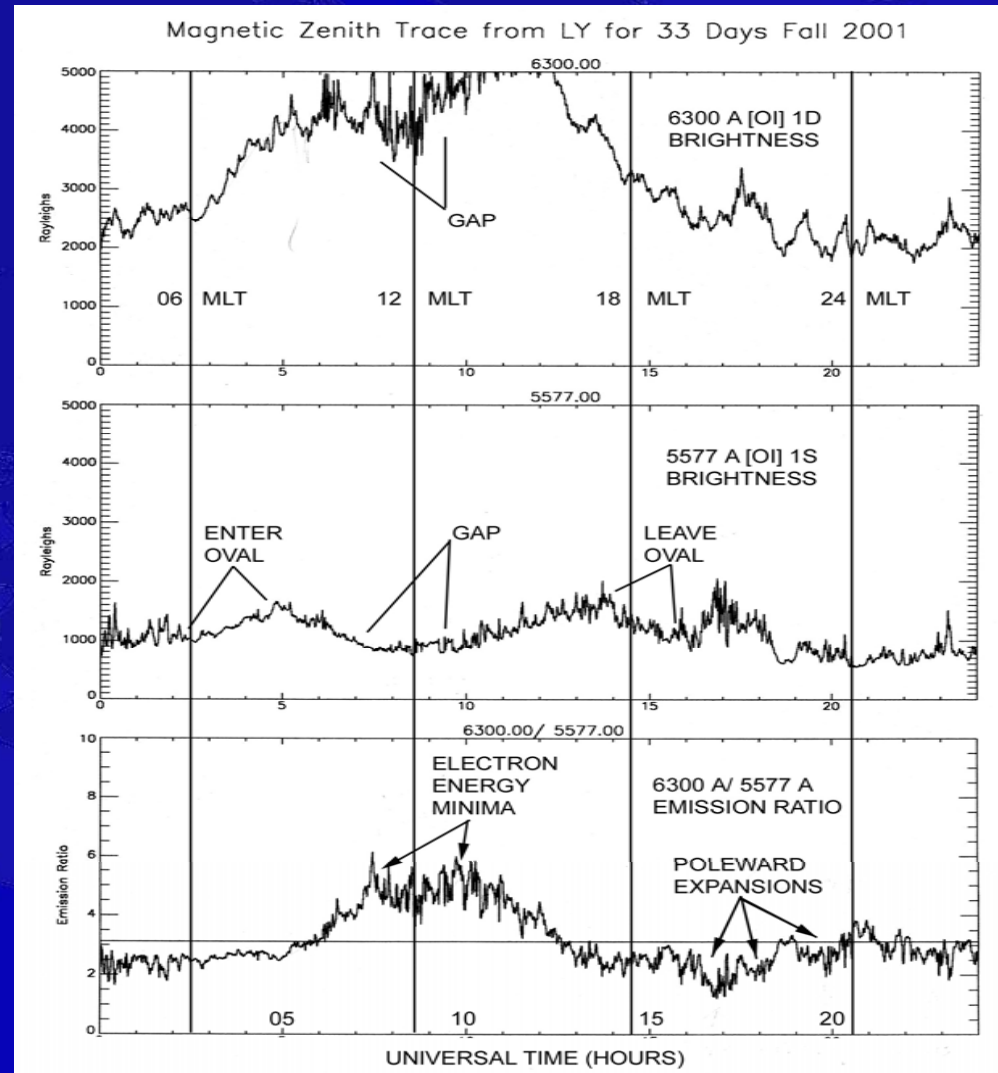
Hypothetical Convection Pattern

- IMF $B_z < 0$.
- 5 different types of auroral forms associated with convection pattern.
- LYR moves under the convection pattern S of the station shown here.



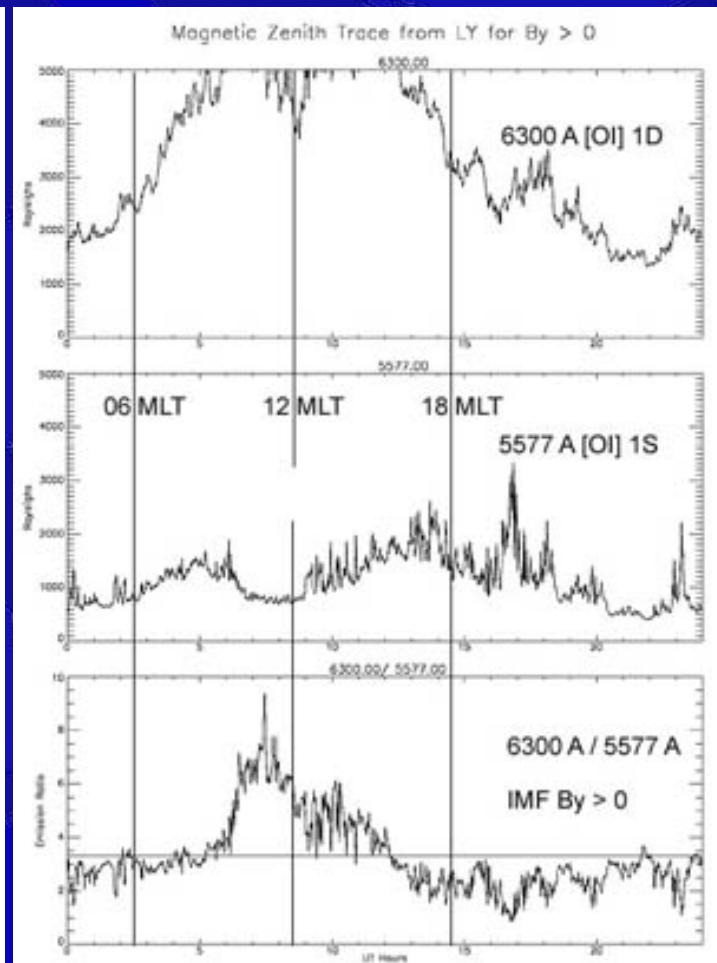
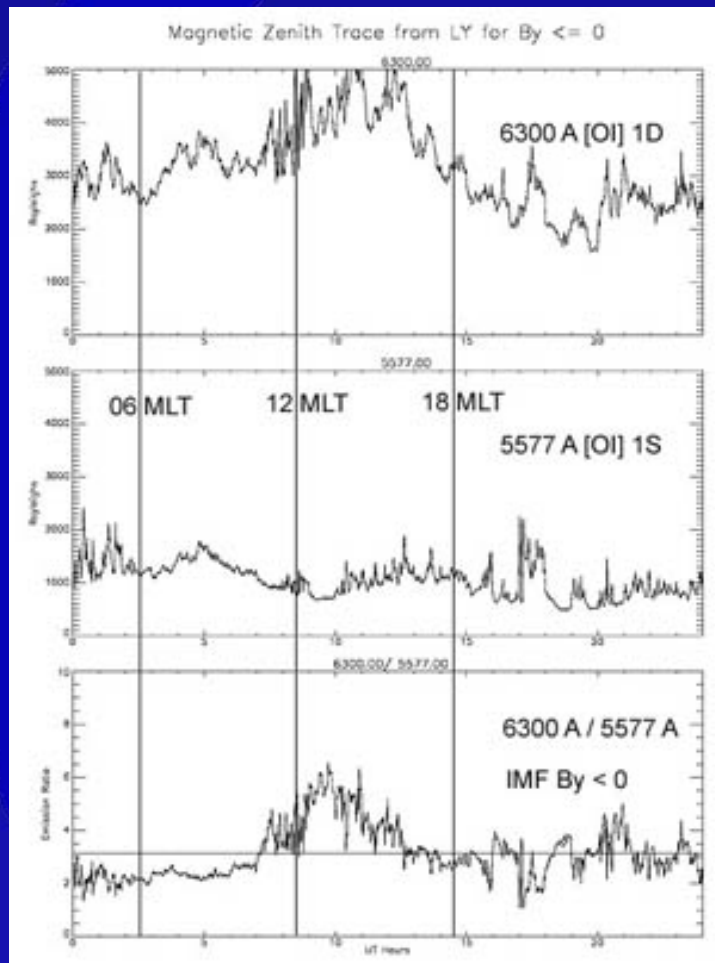
The Dayside Gap

- Gap in dayside aurora is shown to be diminished 5577 A emission.
- 6300 A shows a slight gap also.
- 6300 A/5577A ratio inversely proportional to incoming electron energy.
- Minimum energy around magnetic noon.



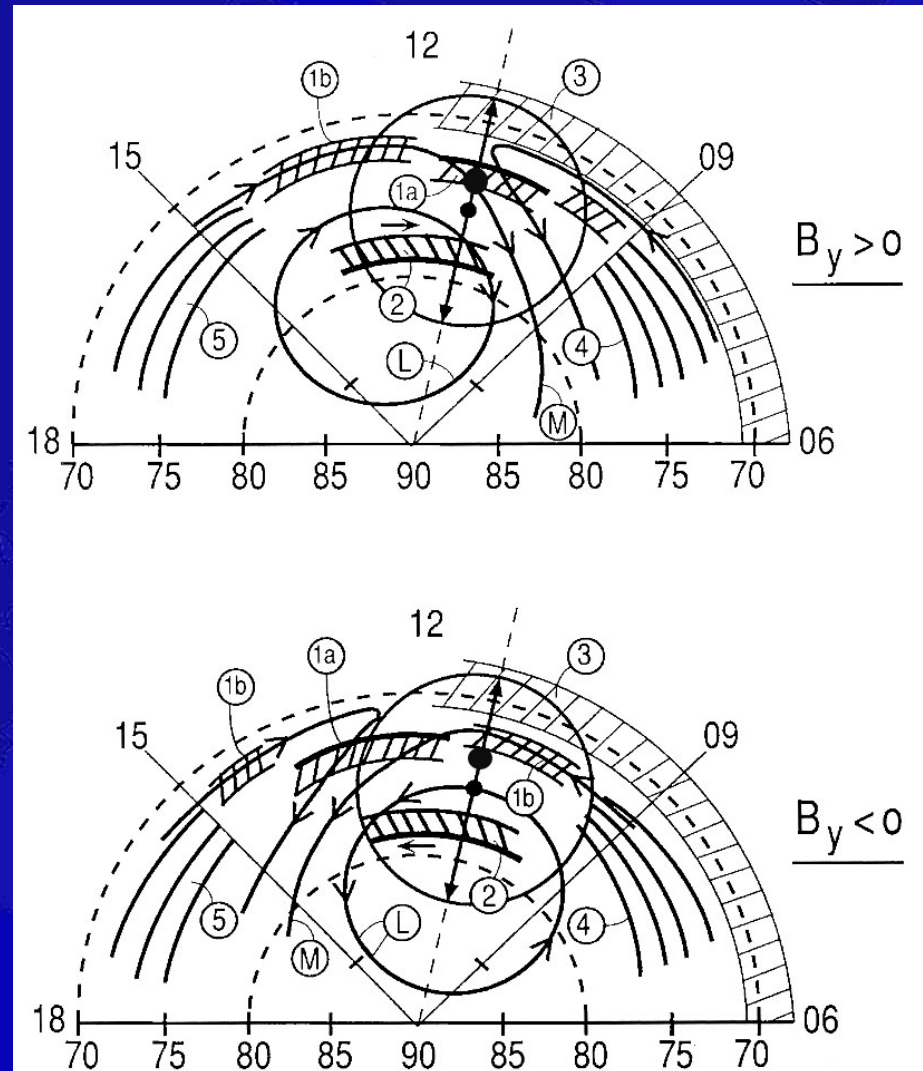
IMF Effect on Dayside Gap

- 6300 A/5577A ratio inversely proportional to incoming electron energy.
- Minimum energy in afternoon for $B_y > 0$, in the morning for $B_y < 0$



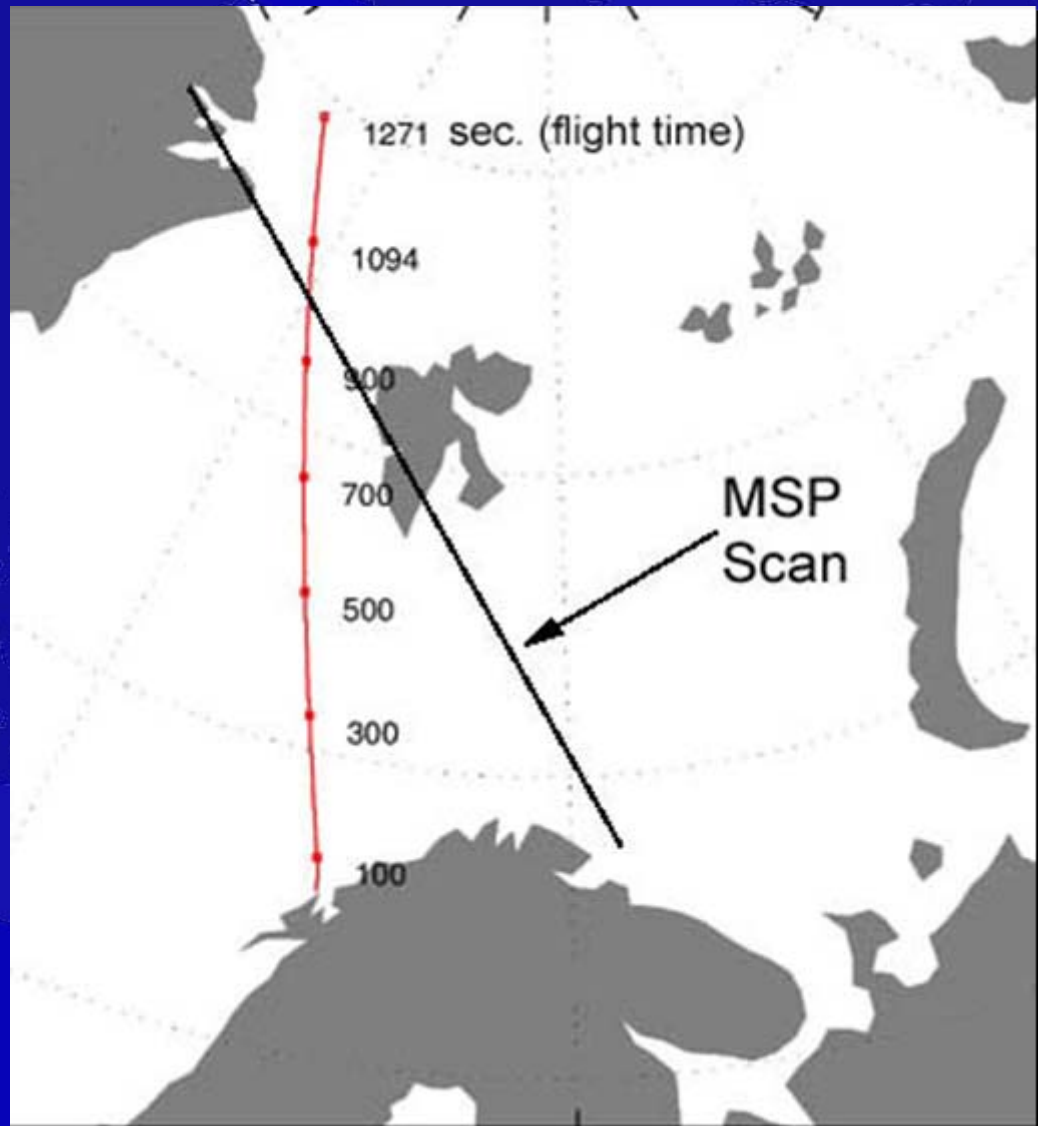
Hypothetical Convection Pattern

- IMF $B_z < 0$.
- 5 different types of auroral forms associated with convection pattern.
- Type 1a in the convection throat is less energetic than type 1b in the merging line



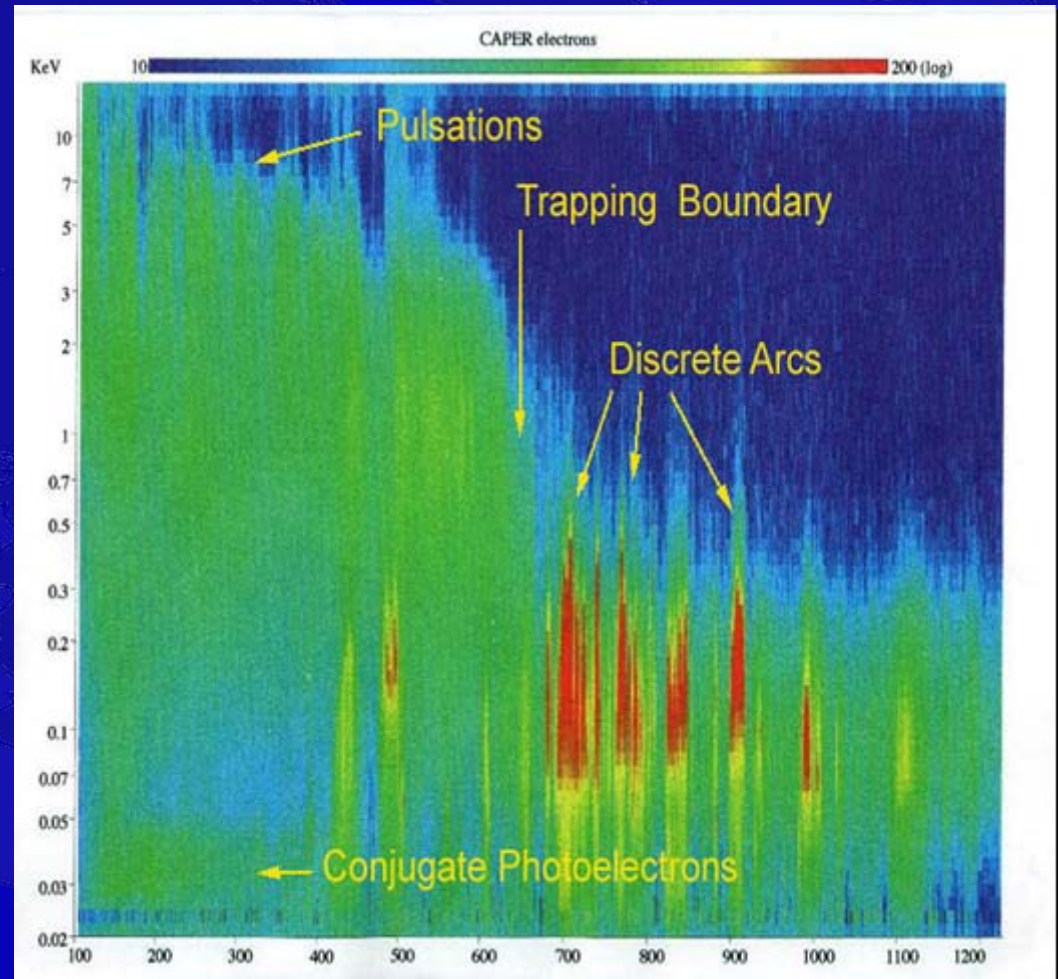
CAPER Trajectory

- Flew West of planned trajectory over LYR.
- As with SCIFER, the 140 km conjugate position was linked to the MSP scan along constant L shells for comparison.

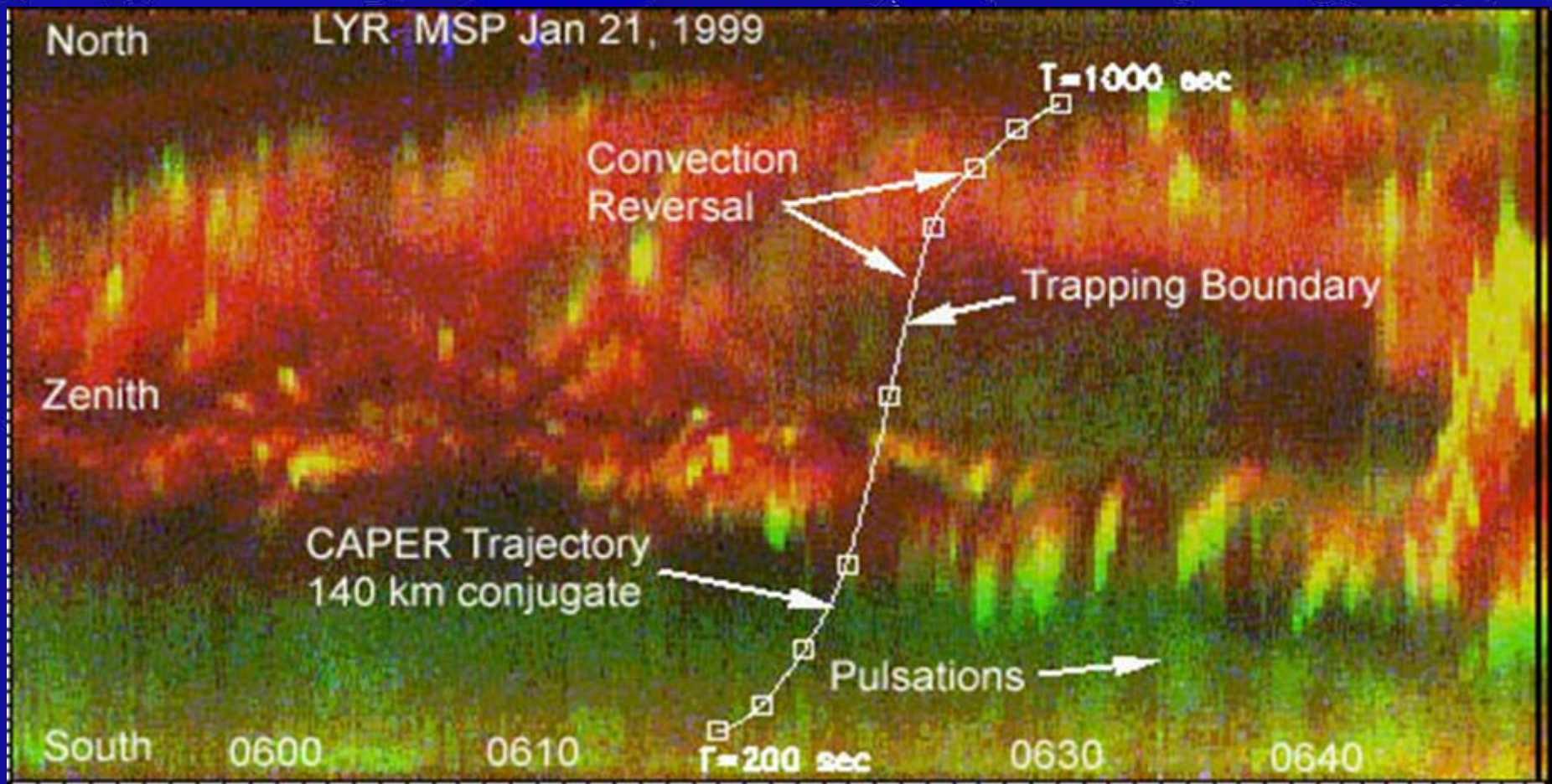


CAPER Energetic Electron Flux

- CAPER similar to SCIFER.
- Except
 - discrete forms both equatorward and poleward of TB.
 - Conjugate photoelectrons end short of TB.



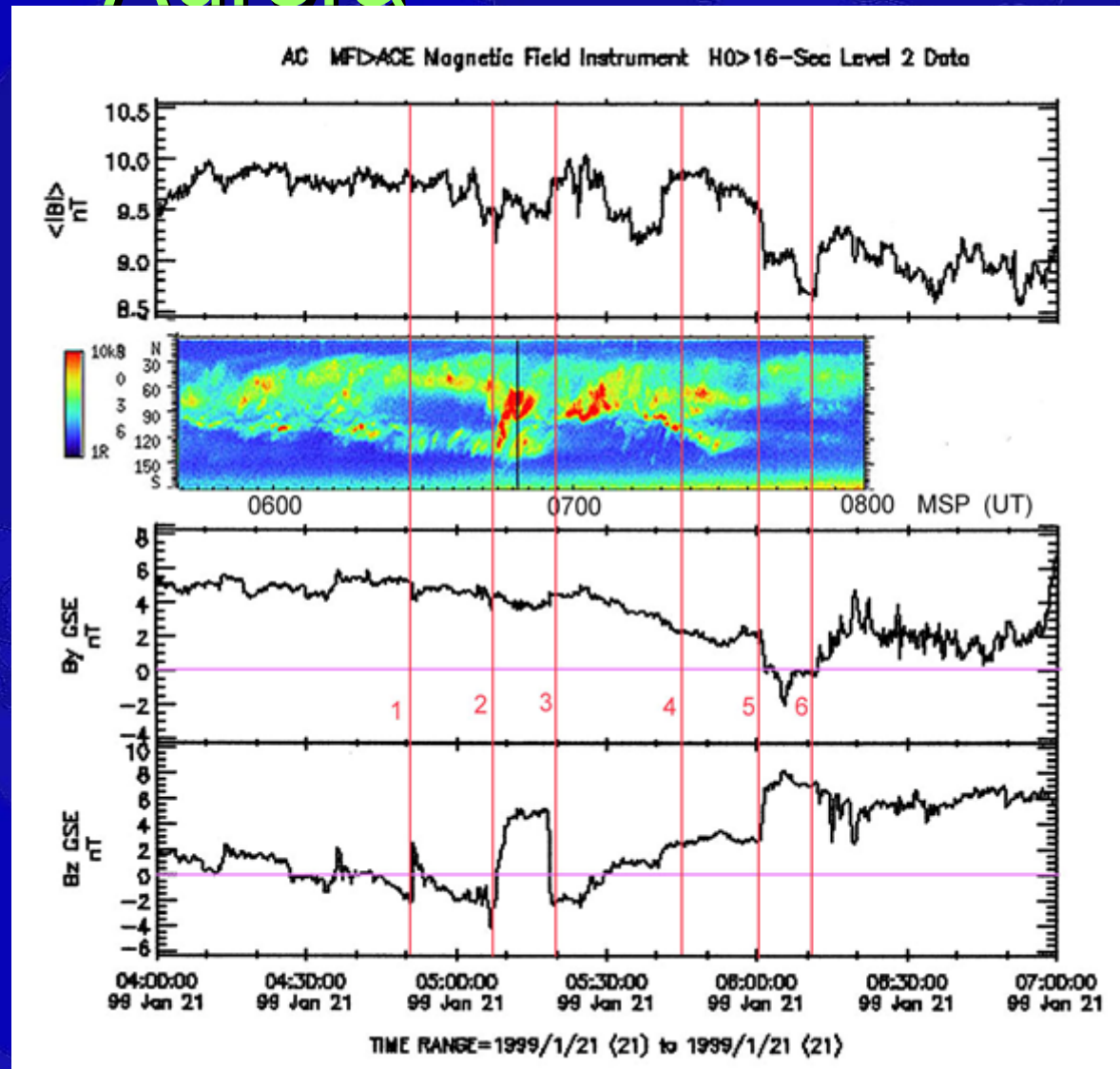
CAPER Meridian Photometer



- Discrete forms on poleward and equatorward side of TB.
- Pulsations on equatorward side of TB.

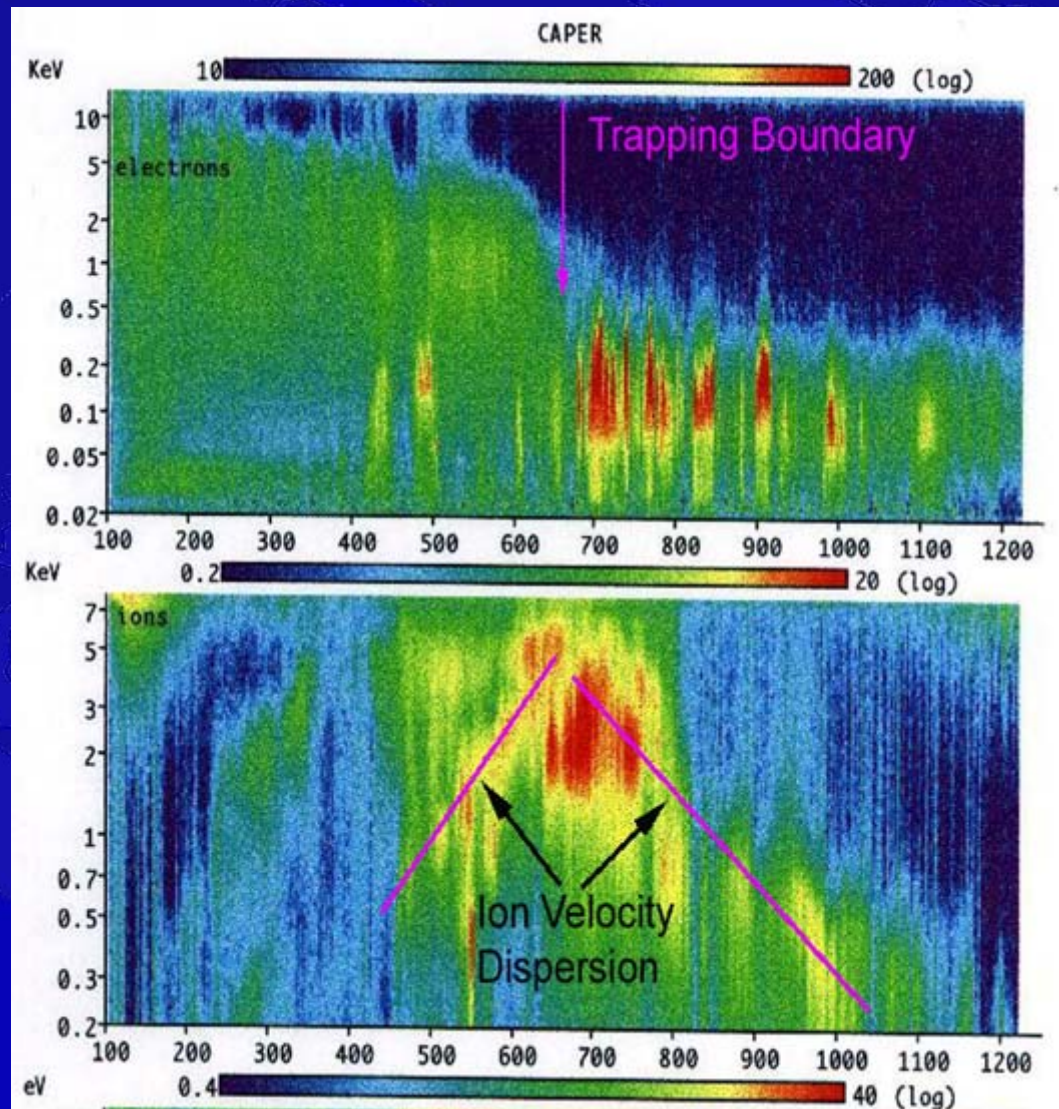
IMF B Variations & Optical Aurora

- IMF Bz near zero.
IMF By positive.
- Two discrete arc regions separated by trapping boundary.
- Northward turning Bz produces forms in both regions at 0640 UT.
- Southward turning near 0700 UT produces form poleward of TB.



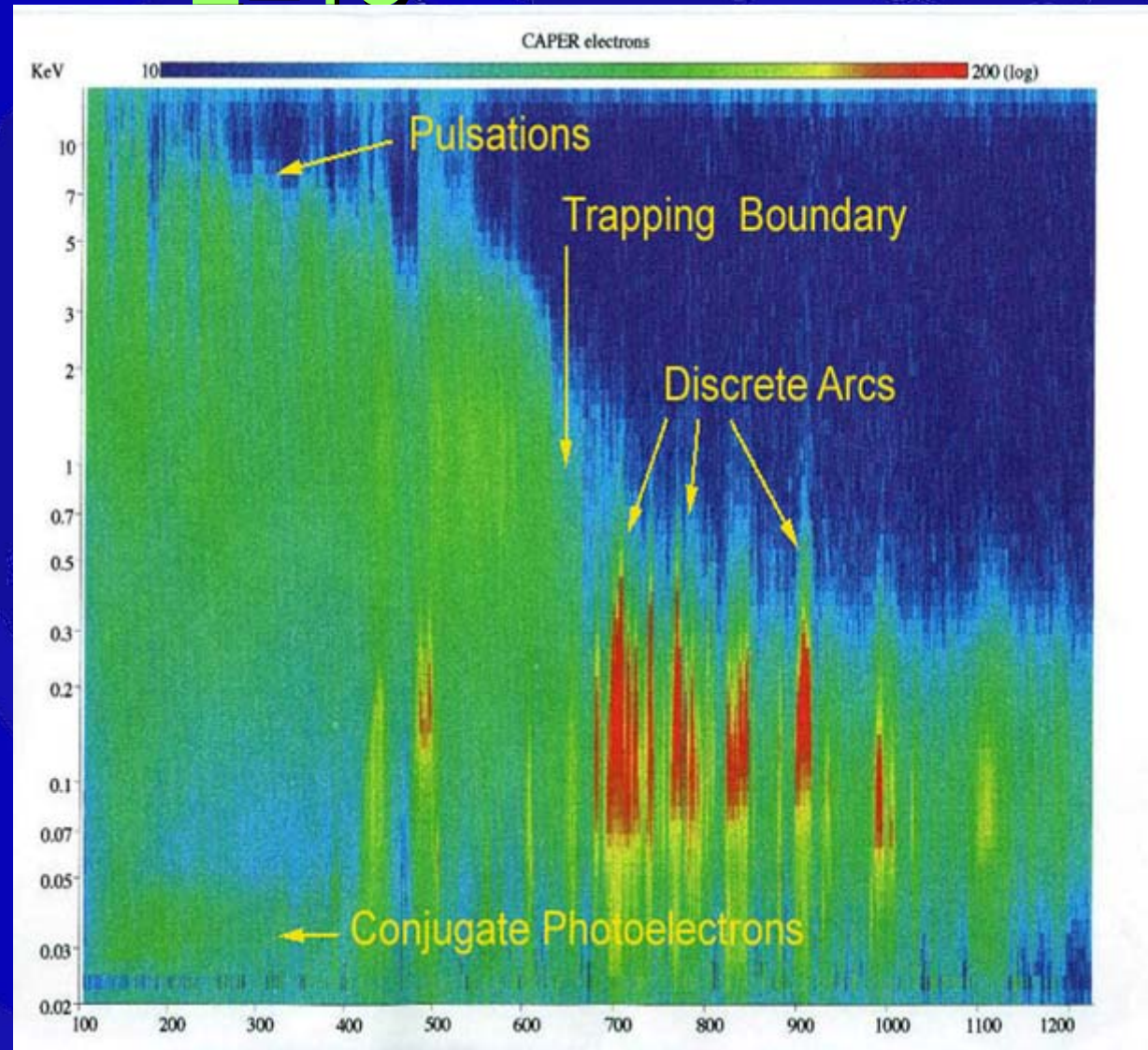
CAPER Ion and Electrons

- Origin of auroral forms in the two regions is found in the particle data.
- Ion velocity dispersion indicates convection in two directions from the TB.

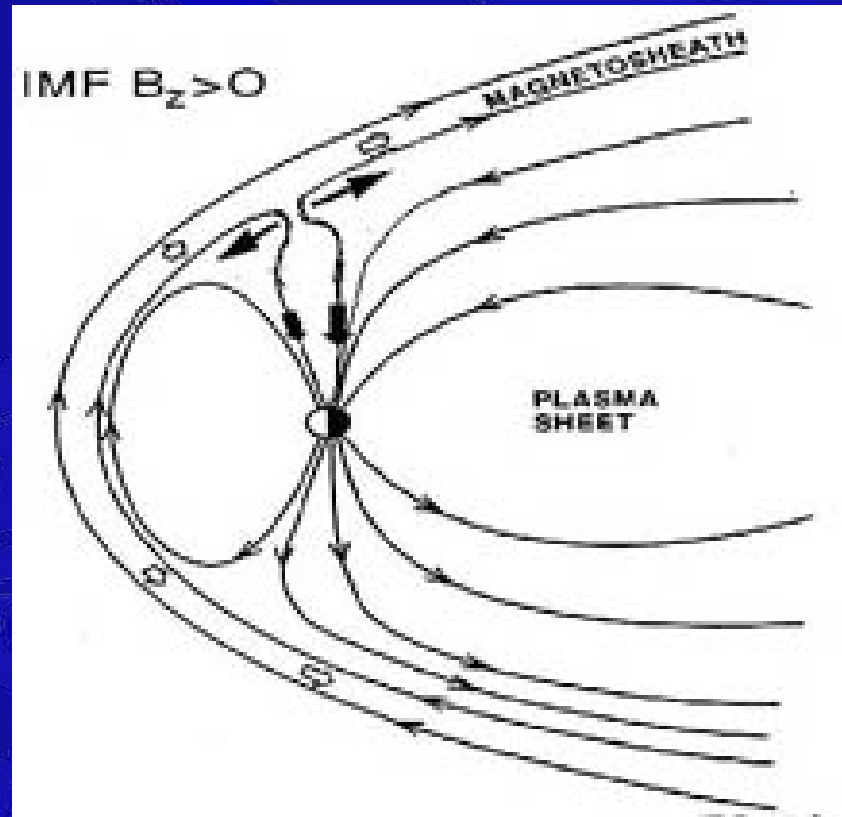
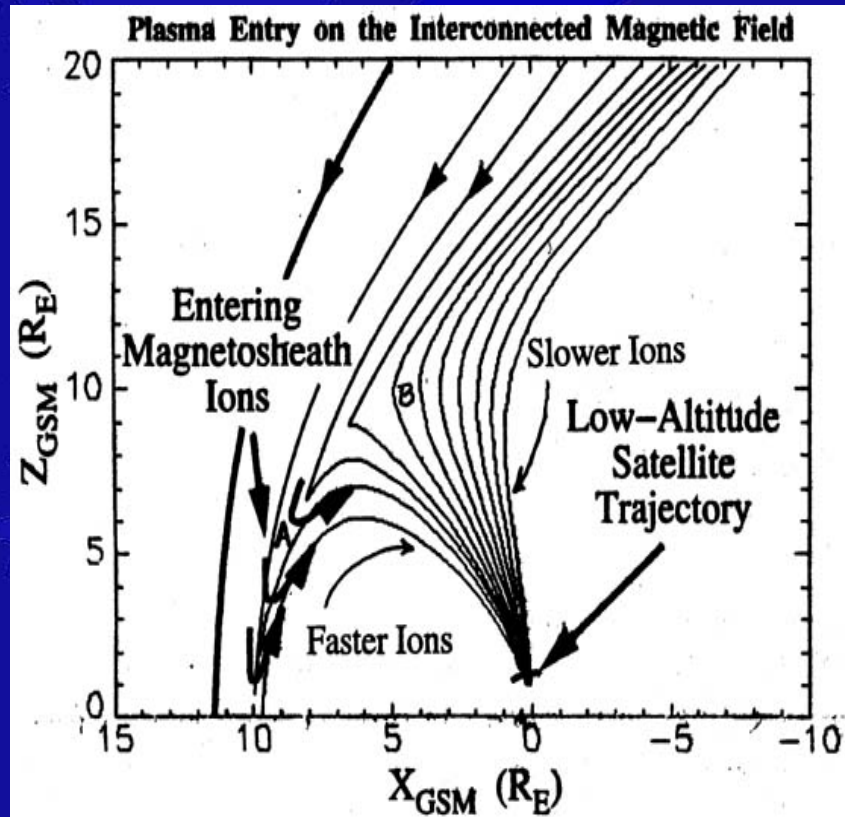


Conjugate Photoelectrons to $L=15$

- Non-local photoelectrons on both flights in dayside aurora.
- Photoelectron transport from conjugate region observed to $L=15$
- Field lines equatorward of discrete aurora are closed and dipolar.



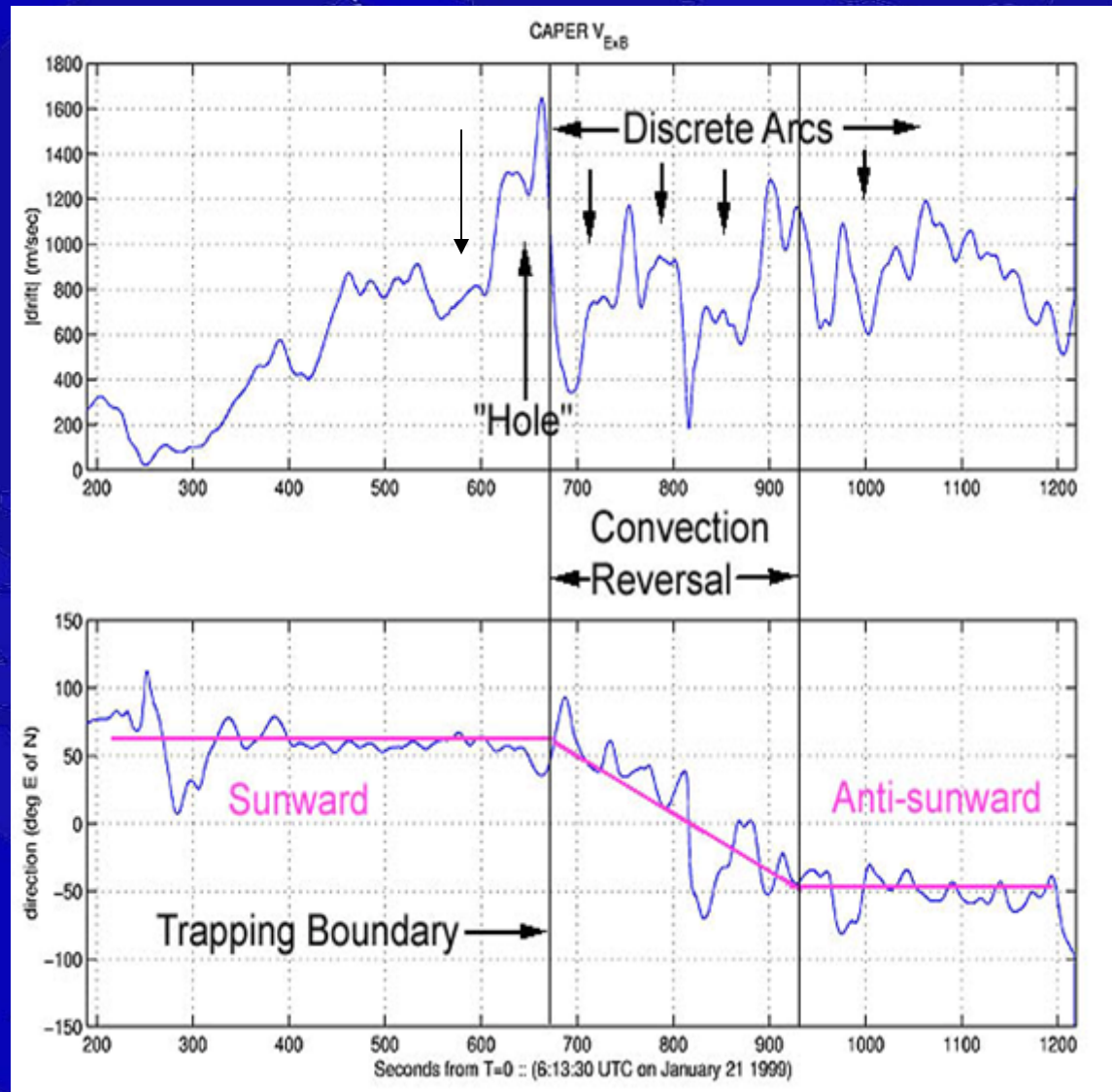
Dayside Merging



- SCIFER IMF $B_z < 0$
- CAPER IMF $B_z > 0$
- Newly open field lines
- Newly closed and opened

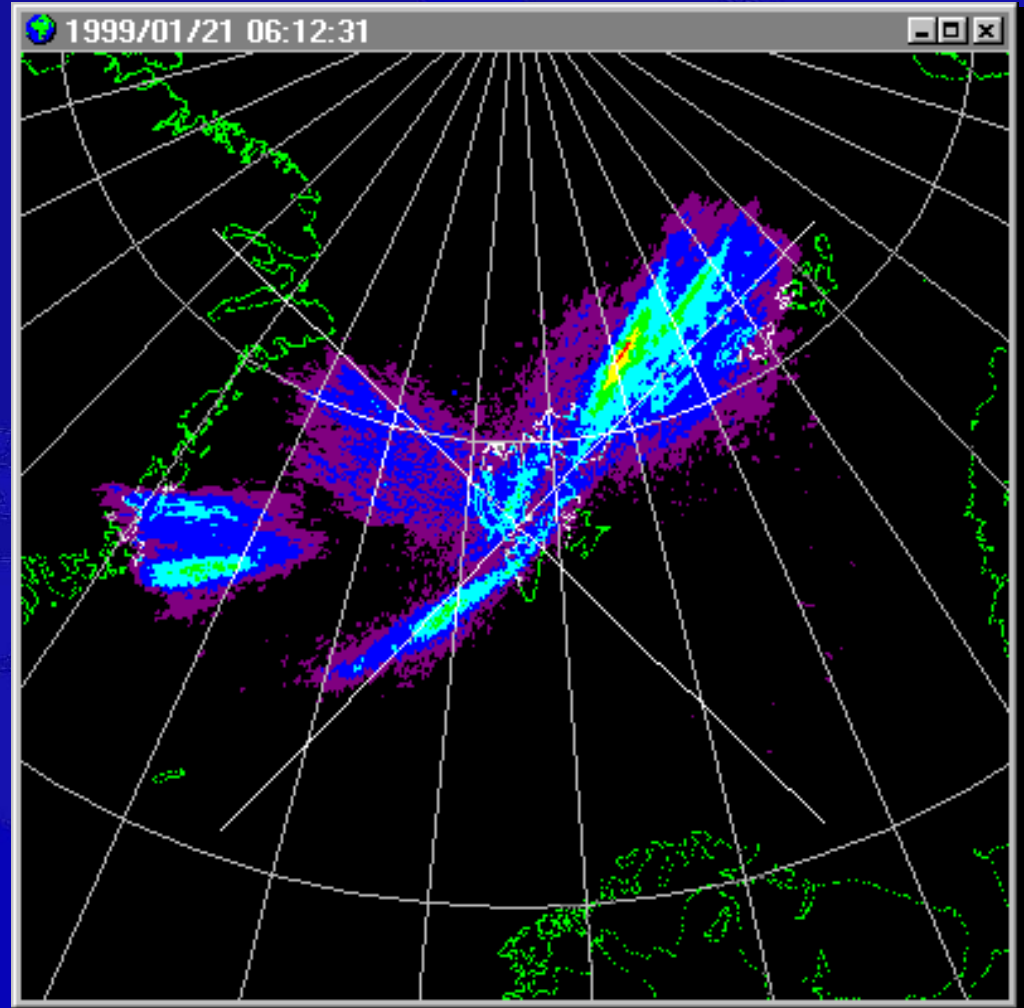
CAPER Convection Velocity

- Sunward convection equatorward of TB.
- Anti-sunward convection poleward of TB.
- Fastest speed between arcs.
- CAPER showed broader convection reversal region than SCIFER.

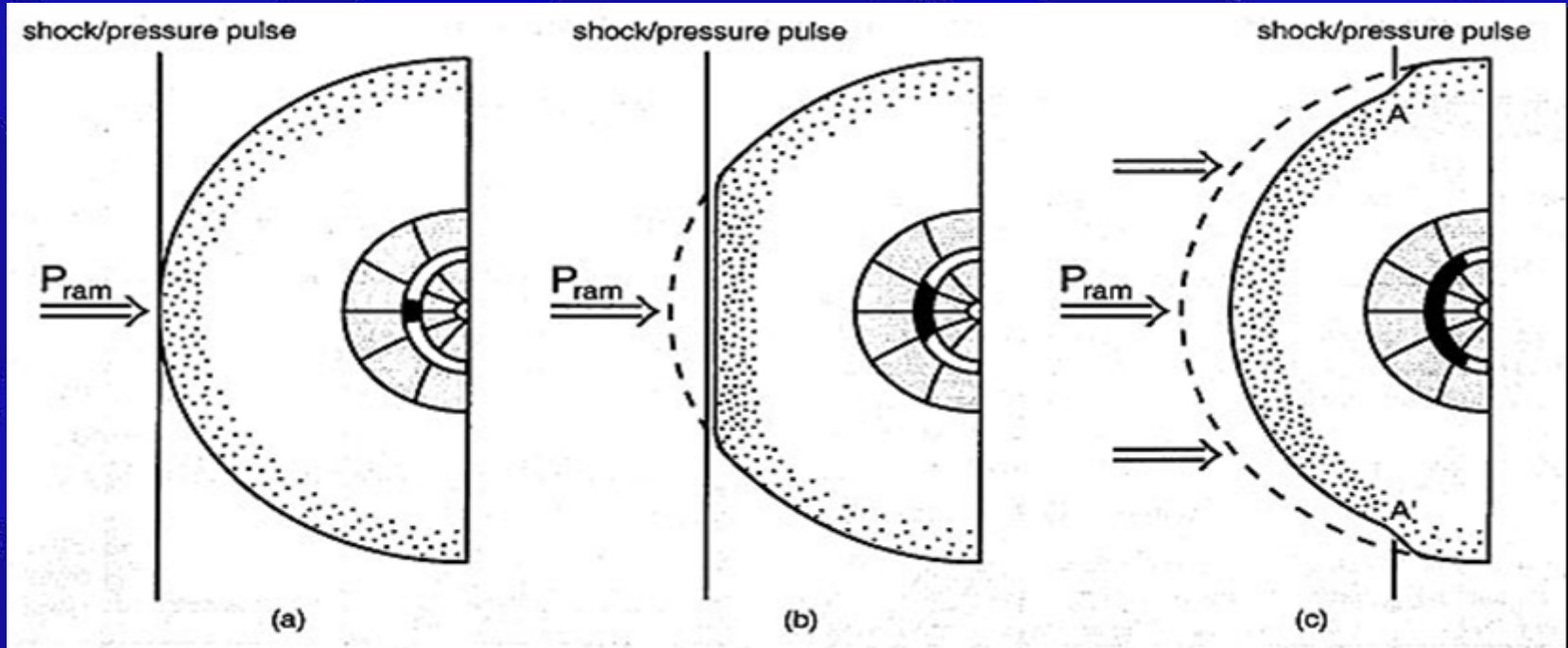


“CAPER” Rocket Observations

- Motion of convection is E-W along the auroral forms.
- Equatorward forms show sunward convection motion.
- Poleward forms show anti-sunward convection motion.

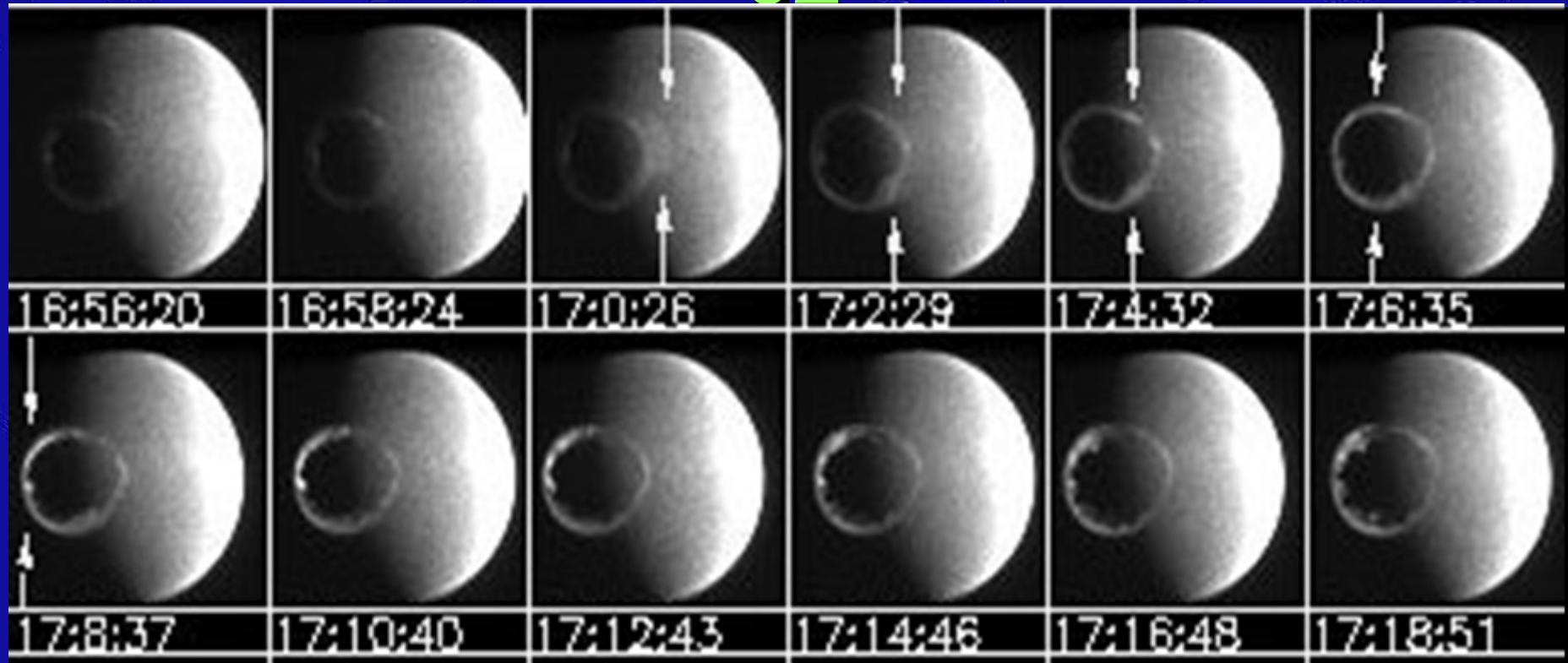


Pressure Pulse Aurora



- Speed of pulse along the magnetopause is consistent with 15 km/sec advance of aurora.

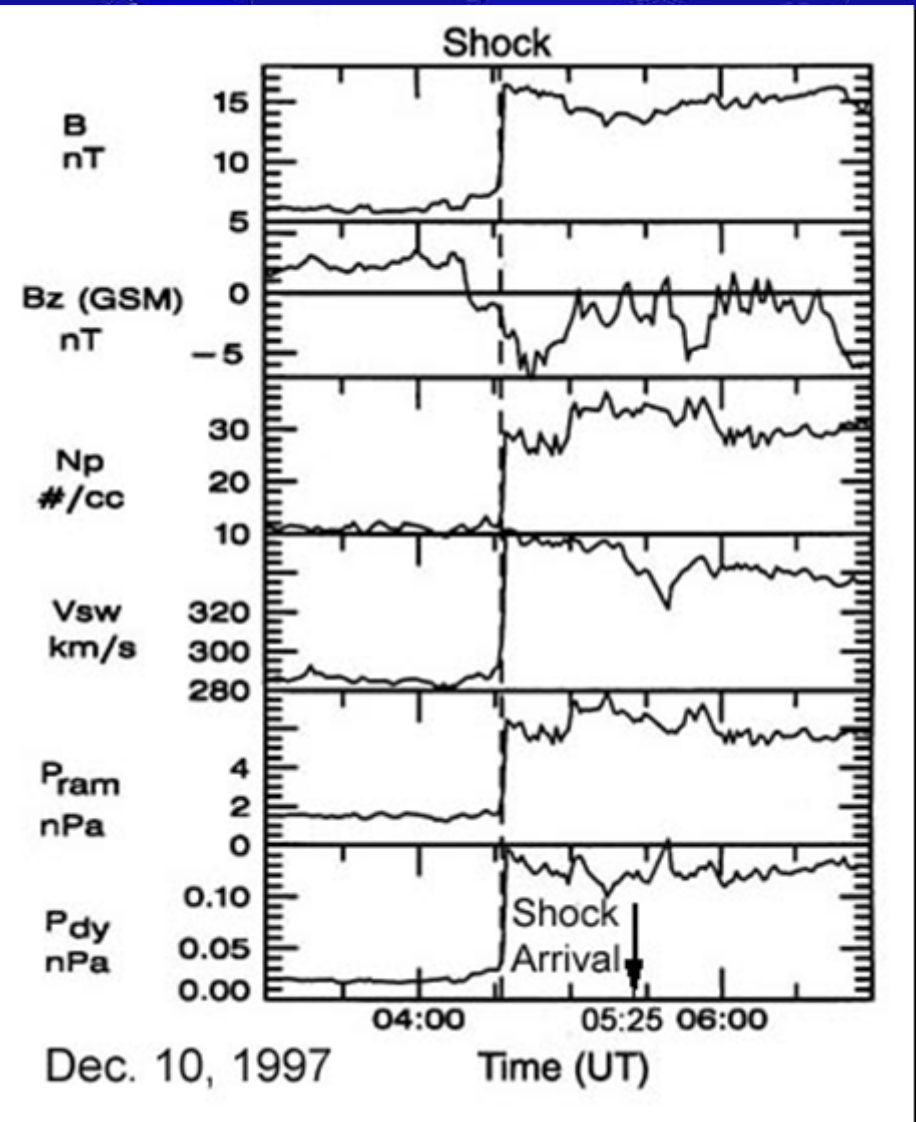
Solar Wind Shock Arrival, Oct 21, 02



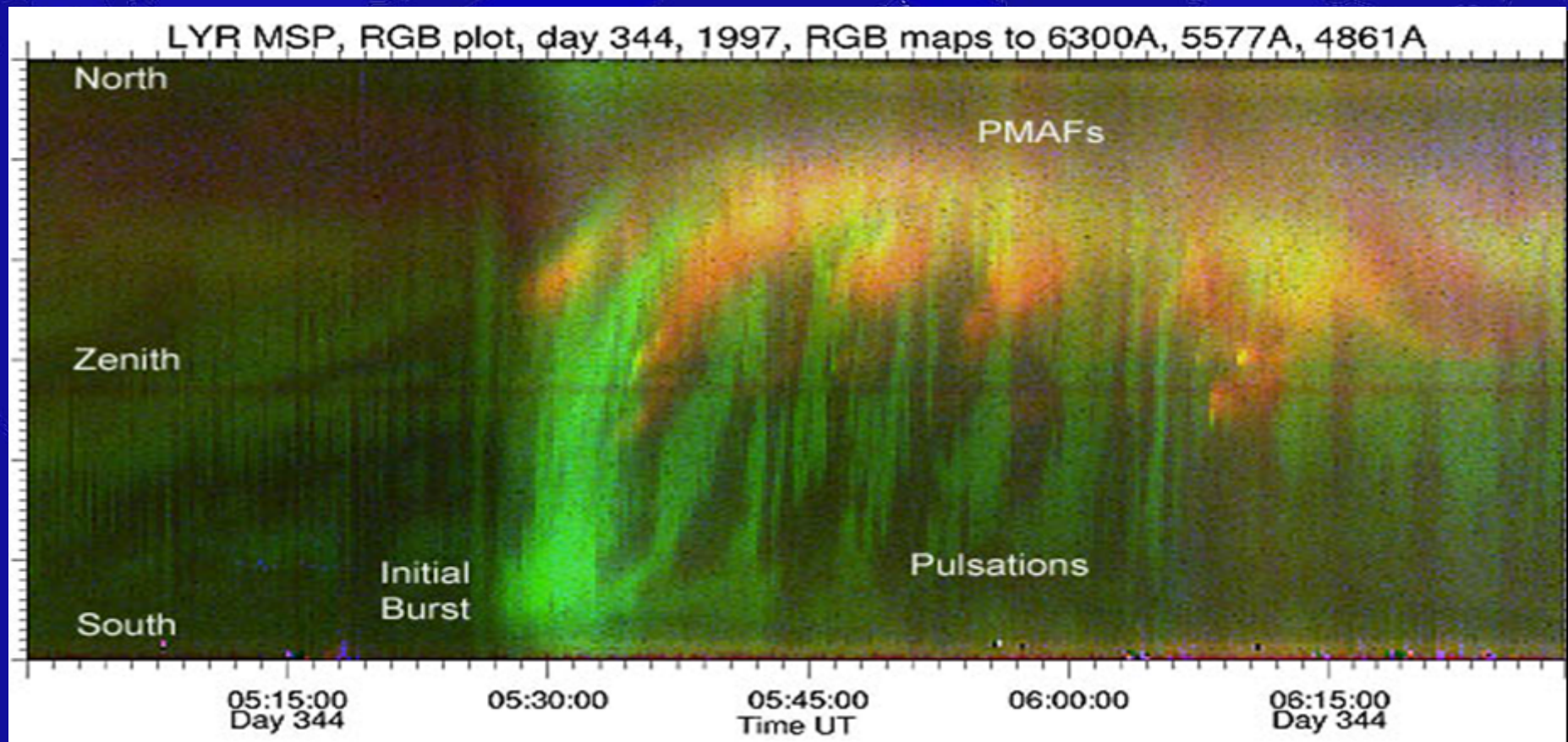
- Large area of luminosity equatorward of oval at 17:00:26 UT
- Two minutes later moved to 10am and 2pm.
- Reached midnight in 8 minutes.

Solar Wind Shock Dec. 10, 1997

- WIND satellite observed shock in the solar wind at 04:30 UT.



Dayside Pressure Pulse Aurora



- Initial aurora from pressure pulse is equatorward of TB.

Pressure Pulse Aurora

- Polar UVI observations of pressure pulse aurora .
- Red dots show ground stations:
 - LYR at 0900 MLT observed diffuse electron aurora.
 - PKR, Ft Smith, Gillam observed H emissions in the evening MLT.
- We conclude that this aurora results from disturbance of gradient drift particles inside the TB by the pressure pulse.

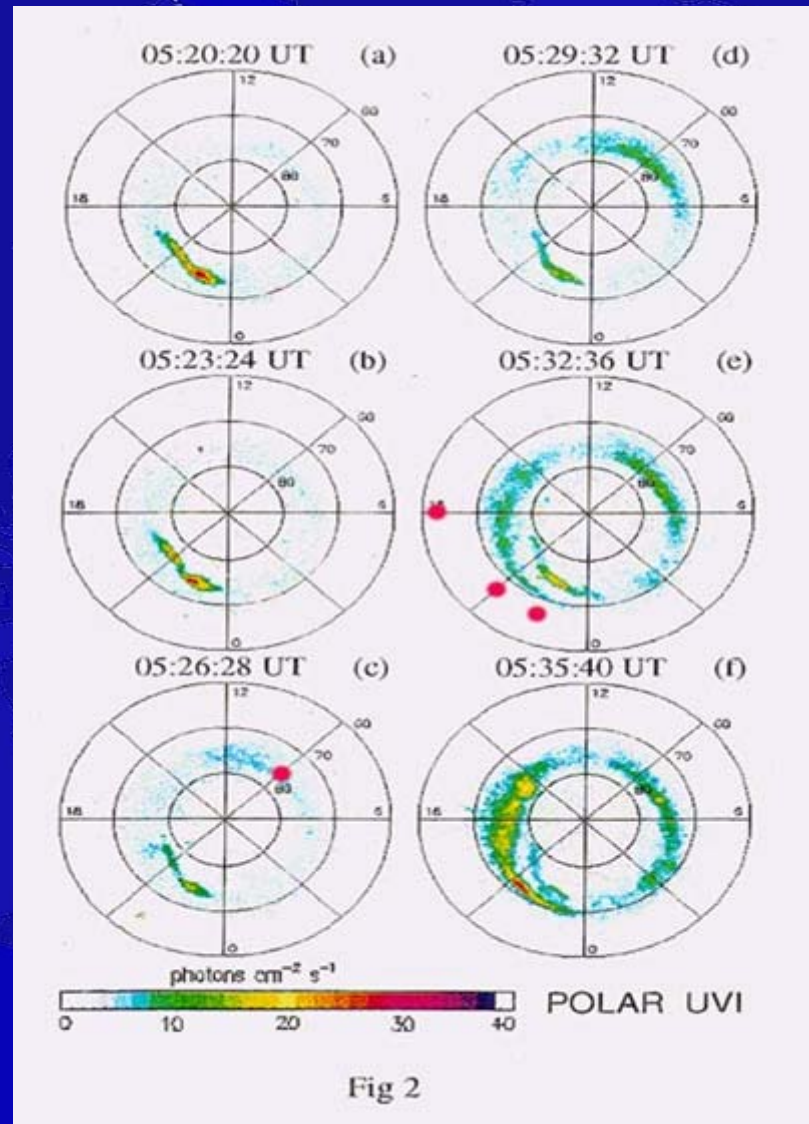


Fig 2

Dayside Magnetospheric Boundaries

